

# A Review of Terminology Used to Describe Soot Formation and Evolution under Combustion and Pyrolytic Conditions

Hope A. Michelsen,\* Meredith B. Colket, Per-Erik Bengtsson, Andrea D'Anna, Pascale Desgroux, Brian S. Haynes, J. Houston Miller, Graham J. Nathan, Heinz Pitsch, and Hai Wang



Cite This: ACS Nano 2020, 14, 12470–12490



Read Online

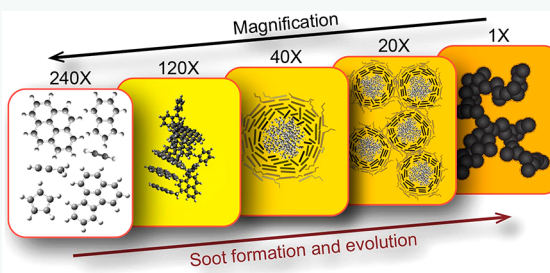
ACCESS |

Metrics & More

Article Recommendations

**ABSTRACT:** This review presents a glossary and review of terminology used to describe the chemical and physical processes involved in soot formation and evolution and is intended to aid in communication within the field and across disciplines. There are large gaps in our understanding of soot formation and evolution and inconsistencies in the language used to describe the associated mechanisms. These inconsistencies lead to confusion within the field and hinder progress in addressing the gaps in our understanding. This review provides a list of definitions of terms and presents a description of their historical usage. It also addresses the inconsistencies in the use of terminology in order to dispel confusion and facilitate the advancement of our understanding of soot chemistry and particle characteristics. The intended audience includes senior and junior members of the soot, black carbon, brown carbon, and carbon black scientific communities, researchers new to the field, and scientists and engineers in associated fields with an interest in carbonaceous material production *via* high-temperature hydrocarbon chemistry.

**KEYWORDS:** soot, particles, particulates, inception, nucleation, incipient, nascent, agglomeration, aggregation, carbonization



Scientific progress in any field relies on the communication of hypotheses, methods, assumptions, approximations, results, and conclusions. A lack of precision in technical terminology can hinder communication, generate confusion, and slow progress. This problem is particularly difficult to avoid in broad, multidisciplinary fields, where terms appropriated from other fields may have ambiguous meanings in a different context. With this perspective, we have undertaken a review of the terminology employed in the study of the production and evolution of soot. Although the focus of this review is on combustion-generated soot, much of the terminology also applies to carbonaceous particle nucleation and growth under pyrolytic conditions.

Knowledge of combustion-generated particles has grown and evolved over the decades with the continuous advancement of both experimental and numerical investigative tools. The ongoing discovery of new details has led to the progressive introduction of new terminology to describe them. This process has tended to be *ad hoc*, resulting in a number of inconsistencies and ambiguities, perhaps augmented by cross fertilization by researchers from disparate disciplines with different terminology to describe the same phenomenon. An

additional important factor is that soot is not a uniquely defined material in size, morphology, or composition. The objective of the present review is therefore to address these inconsistencies and increase the precision of our terminology, with a view to advancing our understanding of soot chemistry and particle characteristics.

The need to clarify terminology related to soot formation and evolution was discussed during the fourth International Sooting Flames Workshop, which took place in July 2018 in Dublin, Ireland.<sup>1</sup> This review addresses this need by presenting a glossary of terminology that we believe is currently in use. Where appropriate, we have compiled brief histories and definitions of the terms frequently used to describe soot formation and evolution during combustion. Where there is

**Received:** July 25, 2020

**Accepted:** September 28, 2020

**Published:** September 28, 2020



ambiguity about the meaning of a word, we recommend guidelines for future usage. We prefer definitions that address the processes that physically control the particles and the physical characteristics of the particles themselves, as opposed to the sensitivity of various diagnostic approaches. Interpretations of data and implementation-based sensitivity of diagnostic techniques can change with time or between different researchers, but the physical characteristics of the particles, generated by a given process, do not. Defining terms relative to soot evolution facilitates developing a better understanding of the properties of the particles as they evolve and the processes that drive that evolution. We have, however, included a few operational terms that are particularly relevant to the field. We have avoided introducing new alternative expressions.

Overall, soot formation proceeds continuously from gas-phase hydrocarbon molecules to carbonized, aggregated particles. Because of the vast number of molecular changes in this process, it is customary to describe the overall process in terms of a series of simplified stages, as summarized in Figure 1. The distinction between these stages is somewhat arbitrary,

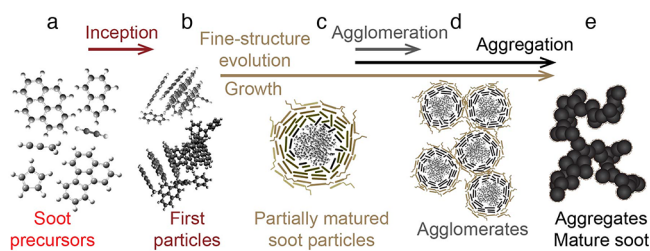


**Figure 1.** Schematic diagram of the major steps in soot formation and the representative species produced as the process proceeds. The relative scale of these images changes between the panels, with the structures ranging from <1 nm (a) to ~100 nm (e).

in that there is no sharp transition, except perhaps for the initial transition between gas-phase and condensed-phase species. Furthermore, the relative importance of each stage depends on local combustion conditions (equivalence ratio, temperature, time, and pressure), together with the associated controlling chemistry. In this context, it is not surprising that some descriptive terms have become ambiguous and in need of clarification.

The first steps in the soot-formation process involve the production of gas-phase hydrocarbon soot-precursor species (Figure 1a), followed by the transition of these species to condensed-phase particles (Figure 1b). Experimental evidence suggests that these first particles are probably liquid-like<sup>2–8</sup> and have limited absorption in the visible spectrum.<sup>9–13</sup> The process of this gas-to-condensed-phase transition is termed “particle inception” or “soot inception”, but the first particles formed (Figure 1b) cannot yet be classified as mature, solidified, and carbonized soot particles. During soot inception, the incipient soot particles thus formed undergo rapid growth by both coagulation and gas-to-particle conversion. They also lose hydrogen through a high-temperature carbonization process, becoming partially graphitic (Figure 1c). As they undergo this carbonization process, their optical properties evolve, such that they become able to absorb and emit light in the visible and near-infrared spectral regions, their density increases, and their surface reactivity may also change. As particles continue to evolve, they collide and form loosely

bound agglomerates of quasi-spherical primary particles (Figure 1d), which eventually become firmly bound, branched-chain aggregates of primary particles (Figure 1e).<sup>14–20</sup>

A series of terms have been developed to describe the chemical and physical evolution associated with each of these stages. However, because the relative importance of each of these processes depends on the combustion environment, the prevailing terminology tends to differ somewhat between groups who target types of flames or combustion processes that produce soot with differing characteristics. In addition, many of these terms are ambiguous. For this reason, we have sought to identify the most prevalent terms and organize the associated discussion according to the most common usage. We have also aimed to ensure consistent terminology related to (1) combustion environments within a flame, (2) pyrolysis environments, including those tailored to generate specific products (e.g., carbon black), and (3) particulate pollutant emissions under conditions relevant to combustion exhaust streams, pool fire and wildfire plumes, and atmospheric evolution (*i.e.*, black and brown carbon, elemental and organic carbon, smoke, and aerosol).

## PAPER STRUCTURE

The terminology discussed in this paper is organized according to the stages of soot formation and evolution. Table 1 gives the section titles in which various terms are defined. The first section, entitled “All Stages”, addresses vocabulary associated with soot in general and is not associated with the characteristics or relevant processes of particles in a single stage. The second section, “Gas-Phase Species”, discusses terms related to the species involved in incipient soot formation and surface growth of particles. The third section, “Transition to First Particles”, introduces terms related to the processes and physical phenomena potentially involved in the transition from gas-phase precursors to condensed-phase particles. The fourth section, “First Particles”, provides a glossary of terms used to describe the particles initially formed from gas-phase precursors. The fifth section, “Particle Growth”, introduces terminology used to describe processes possibly responsible for the growth of particles during their evolution after inception. The sixth section, “Chemical Evolution”, defines terms used to discuss physical properties of particles in different stages of evolution, general classifications of particles as they age, and the chemical processes responsible for changes in their properties. The seventh section, “Relevant Forms of Carbon”, provides a glossary of the phases of carbon, some of which are not generally formed during combustion or only under special conditions but are listed for comparison. We placed this section after the sixth section because it is most closely related to the material properties of the particles as they evolve chemically. The eighth section, “Transition to Aggregates”, introduces terms to describe morphological changes in particles as they evolve. The ninth section, “Oxidation and Breakup”, describes terms used for discussing particle depletion by oxidation. The tenth and final section, “Associated Expressions”, presents definitions for terms used for soot in atmospheric science and particle synthesis. It also defines terms used for assessing soot formation with respect to atmospheric emissions.

**Table 1.** Terms Defined in the Paper

all stages	gas-phase species	transition to first particles	first particles	particle growth
particle	soot precursors	inception	incipient soot particles	coagulation
particulate	surface-growth species	nucleation	nuclei	coalescence
soot		condensed phase	nascent particles	surface growth
surface		chemical bonds	nano-organic carbon	condensation
bulk		covalent bonds	growth centers	vaporization
mechanism		van der Waals interactions	clusters	evaporation
		dispersion forces	liquid-like particles	boiling
				deposition
				sublimation
				physisorption
				chemisorption
				adsorption
				desorption
chemical evolution	relevant forms of carbon	transition to aggregates	oxidation and breakup	associated expressions
graphitization	amorphous carbon	primary particles	oxidation	black carbon
carbonization	graphene	agglomeration	fragmentation	brown carbon
annealing	graphite	agglomerates		elemental carbon
soot aging	turbostratic graphite	aggregation		organic carbon
maturity	polycrystalline graphite	aggregates		Ångström exponent
maturity level	glassy carbon	super-aggregates		carbon black
young soot particles	diamond	dendritic		carbon nanoparticles
partially matured particles	fullerenes	ramiform		aerosol
partially graphitized particles	carbon onions	ramified		smoke
mature soot particles	carbon nanotubes	morphology		smoke number
fine structure		fractal dimension		smoke point
basic structural unit		restructuring		sooting threshold
dispersion exponent		sintering		threshold sooting index
black-body radiation				yield sooting index
				nonvolatile particulate matter
				volatile particulate matter

## TERMINOLOGY

**All Stages. Particle and Particulate.** These terms are interchangeable. In the context of this discussion, a particle is defined as a small entity of solid or liquid matter distinguishable from the gas phase *via* such properties as density, specific heat, and the optical properties of scattering and absorption cross sections.

**Soot.** “Soot” refers to carbonaceous particles formed during the incomplete combustion or pyrolysis of hydrocarbons, including incipient soot particles, mature soot particles, and all of the intermediate particulate stages between inception, maturity, and complete oxidation to gas-phase species. This term also refers to species emitted from a flame and into the exhaust stream or outlet from a reactor.

**Surface.** The particle surface is the first layer or first few layers of atoms or molecules physically or covalently bound to the particle at the interface between the particle and the gas phase.

**Bulk.** The particle bulk is the rest of the particle that is not at the surface.<sup>21,22</sup>

**Mechanism.** In combustion science, the word “mechanism” is frequently used to describe a set of elementary reactions involving multiple reactants and products, together with the corresponding rate coefficients compiled for inclusion in chemical kinetics models or reaction models. In chemistry, “mechanism” is used to describe a detailed chemical-reaction pathway or set of pathways leading from reactants to products.<sup>23–25</sup> “Mechanism” may also refer to a set of gas-surface reactions at the particle interface or to detailed

chemical pathways occurring at the particle surface (at any particle-maturity level), leading to soot mass growth or oxidation; see the Chemisorption section.

**Gas-Phase Species. Soot Precursors.** Soot precursors are molecular gas-phase species that serve as the molecular building blocks of soot particles. They play a role in particle inception and mass/size growth. The specific species leading to soot inception have not been definitively identified. There could be many different soot precursors with roles that depend on local flame conditions. Early models assumed these species to be small hydrocarbons, such as acetylene and benzene.<sup>26–28</sup> These and other models use surrogates for molecular species involved in the particle inception process, largely because of a lack of knowledge of the actual species, uncertainties in their kinetics, variations caused by investigation with different fuels or combustion conditions, and computational limitations. Potential candidates for precursors that drive inception include unsubstituted polycyclic aromatic hydrocarbons (PAHs),<sup>19,29–32</sup> aliphatically bridged<sup>9,33–40</sup> or substituted PAHs,<sup>31,33,35,38–40</sup> ions,<sup>15,41,42</sup> radicals,<sup>19,23,39,40,43,44</sup> and oxygenated hydrocarbons.<sup>9,35,45,46</sup> The expression “soot precursor particles” is sometimes used to refer to incipient or young soot particles as a precursor to mature soot aggregates,<sup>47–54</sup> but we recommend restricting the use of “soot precursors” to refer to gas-phase species.

**Surface-Growth Species.** Surface-growth species are gas-phase molecular species that chemisorb, physisorb, condense, or deposit to or on the particle surface, thereby adding mass to the particle. Early experimental results suggested that acetylene

was a likely candidate for driving mass growth of particles in flames at atmospheric and lower pressures.<sup>55,56</sup> Hydrogen atoms are also argued to play a role, *via* the hydrogen abstraction C<sub>2</sub>H<sub>2</sub> addition (HACA) mechanism, in maintaining the surface activity.<sup>57</sup> Hydrogen atoms or molecules may be released as part of the surface-growth process. Depending on the fuel and the flame environment, other species (*e.g.*, acetylenic species, aromatics, PAHs, and radicals) may contribute, either by chemisorption, physisorption, condensation, or deposition;<sup>22,23,58–61</sup> see the **Surface Growth, Adsorption and Desorption, Chemisorption, Physisorption, Condensation, and Deposition** sections.

**Transition to First Particles. Condensed Phase.** Although “condensation” generally refers to the phase transition of gas-phase species to a liquid phase,<sup>62–66</sup> both liquid and solid phases are referred to as “condensed phases”. The phase in which a material is thermodynamically stable depends on temperature and pressure. For example, a substance that is in the condensed phase at room temperature may be in the gas phase at flame temperature. See the **Condensation and Deposition** sections.

**Inception.** The word “inception” was introduced to the field of combustion science in the early 1980s to represent the transition from gas-phase-precursor species to condensed-phase (*i.e.*, liquid or solid) particles.<sup>14,16,18,19,22,23,28,39,53,58,60,67–91</sup> The term was coined to describe gas-to-condensed-phase transitions independently of specific mechanisms. Such a transition occurs when the properties (*e.g.*, density, specific heat, and absorption and scattering cross sections) of the particle or cluster depart from those of the gas-phase species from which it is composed and begin to exhibit properties of a bulk material.<sup>92</sup> The details of this process are poorly understood. This term does not require knowledge of the mechanisms for initial-particle formation or the characteristics of the first particles formed. It has been used extensively in this context over the past four decades. There are still large gaps in our understanding of the mechanisms controlling the transition from the gas-phase precursors to the condensed-phase particles and the characteristics of the “first particles” formed. “Inception” is thus still an appropriate term to represent this process; see also the **Nucleation** section.

**Nucleation.** With respect to soot formation, “nucleation” also refers to the process of particle formation from gas-phase precursors.<sup>6,14–16,18–20,22,27,39,58,60,68,70–72,75–79,81–91,93–99</sup> Although “nucleation” has commonly been used interchangeably with “inception”, it is more usefully distinguished from “inception” as a term that implies condensation or deposition, that is, thermodynamically driven processes leading to particle formation by van der Waals or other interactions. In the context of classical nucleation theory, “nucleation” is exclusively used to describe the competition between the Gibbs free energy as a driving force for condensation and the surface tension that counteracts condensation.<sup>100</sup> “Inception”, on the other hand, encompasses all mechanisms for particle formation,<sup>14,22,39,60,73,76,81,89,95</sup> including thermodynamically driven phase transitions and kinetically driven chemical reactions. Hence, if the microprocesses of how particles are formed are not known or not well-defined, we recommend the term “inception” as it is more general.

**Chemical Bonds.** A chemical bond is an attractive interaction between atoms that is strong enough to form a multiautom complex with distinct chemical or physical character.<sup>101</sup> There are several types of bonds: electrostatic,

covalent, and metallic.<sup>101</sup> The most important of these types for soot formation is the covalent bond; see the **Covalent Bonds** section.

**Covalent Bonds.** A covalent bond is a strong chemical bond formed by the sharing of an electron pair between neighboring atoms.<sup>101,102</sup>

**van der Waals Interactions and Dispersion Forces.** van der Waals interactions are relatively weak electrostatic forces between neutral molecules,<sup>102–105</sup> including radicals.<sup>106–109</sup> The attractive van der Waals forces include dipole attractions between polar molecules, induced dipole attractions between polar molecules and nonpolar molecules, and attractions between nonpolar molecules, the latter of which are known as “dispersion forces” or “London dispersion forces”.<sup>102–105</sup> Dispersion forces are the most important of the van der Waals forces for interactions between PAHs. Furthermore, van der Waals forces can enhance collisional combination of primary particles by a factor of about two.<sup>110</sup> Repulsive van der Waals forces occur at short molecular separations and are due to electrostatic repulsions. A van der Waals complex is a multimolecular structure trapped in a potential energy well, which is a minimum in potential energy with respect to intermolecular distance and orientation; this potential-energy minimum results from the sum of the attractive and repulsive forces.

**First Particles Formed. Incipient Soot Particles.** “Incipient soot particles” are formed at inception.<sup>14–16,18–20,22,23,27,39,53,58,60,67,70,71,76–79,83,85,87–90,96</sup> As with the term “inception”, the expression “incipient soot particles” neither requires nor implies knowledge of the mechanisms by which they were formed (from the gas to the condensed phases) or of their initial characteristics. These terms have been used extensively in this context since their introduction in the early 1980s;<sup>14</sup> see also **Nuclei, Nascent Soot Particles, and Nano-Organic Carbon Particles** sections.

**Nuclei.** The products of nucleation, or inception, are called “nuclei”.<sup>14,19,27,71,72,75,79,83,84,86,93,94,96</sup> The term “nuclei” is often used interchangeably with “incipient particles”. In many other contexts, however, “nuclei” specifically refers to the product of homogeneous nucleation, or self-organizing, which triggers further growth by condensation or deposition. The expression “incipient particles” does not imply a specific formation mechanism. However, those features of mature soot particles exhibiting disordered fine structure, around which more ordered structure is formed, are sometimes referred to as “nuclei” to represent the hypothesis that these particles may have been responsible for initiating the growth of primary particles.<sup>111–113</sup> This definition is synonymous with “growth centers”; see the **Growth Centers** section.

**Nascent Soot Particles.** In combustion science, this expression dates back to the 1970s and is most often used synonymously with “incipient soot particles”.<sup>6,18–20,39,75,80–82,84–87,97–99,114–118</sup> In a limited number of studies, it has been used to indicate young soot, including incipient and partially aged particles.<sup>60,119</sup> “Nascent particles”, “nascent smoke”, and “nascent soot” are also used by atmospheric scientists<sup>120–126</sup> and medical biologists<sup>127,128</sup> to refer to the mature soot particles that exit from a combustor. To avoid confusion caused by the different meanings of this term in different fields, it is preferable to avoid this expression. We suggest instead the use of “incipient soot particles” to refer to the particles formed during inception and a different expression, such as “young soot”, “partially aged soot”,

“partially carbonized soot”, “partially graphitized soot”, or “partially matured soot”, to refer to particles that have evolved beyond the inception stage but have not yet become mature particles.

**Nano-Organic Carbon Particles.** This expression is used to describe small particles with a relatively low molar carbon-to-hydrogen (C/H) ratio. *Ex situ* samples of soot collected from flames suggest that the C/H ratio for these particles is in the range of 1.4–2.5.<sup>16,47,52,59,93,129</sup> These particles are 1–6 nm in diameter,<sup>6,11,12,130,131</sup> spherical,<sup>3,5,6,8,132</sup> liquid-like,<sup>2–8</sup> and nearly transparent in the visible and near-infrared spectral regions.<sup>9–13</sup> They have been shown not to incandesce when irradiated with a laser,<sup>131,133–137</sup> and thus they are not detected with the widely employed laser-induced incandescence (LII) technique, but they do fluoresce upon UV excitation.<sup>131,133,136</sup> The collective evidence to date indicates that these particles are incipient particles, but they may represent a subset of the types of particles formed during inception under different conditions; see the [Incipient Soot Particles](#) section.

**Growth Centers.** Growth centers are disordered or amorphous regions 1–4 nm in diameter located within the central portion of a primary particle.<sup>21,113,138–145</sup> They are consistent with vestiges of incipient particles that may or may not have agglomerated before seeding further particle growth. These features are sometimes referred to as “nuclei”;<sup>111–113</sup> see also the [Nuclei](#) section.

**Clusters.** A cluster is a group of similar objects that are bound together, either tightly or loosely. It may also be a group of a few to thousands of atoms or molecules.<sup>104</sup> Large clusters of molecules may be held together in a nanometer-scale particle that possesses properties in between those of molecular species and bulk matter.<sup>104</sup> In soot science, “cluster” is used to describe a collection of molecular precursor species that form an incipient particle.<sup>6,19,20,23,39,58,75,79,80,82,88,90,96,98</sup> Without defining the inception mechanism, such clusters could be held together by either van der Waals forces or covalent bonds. The term “cluster” is also used to describe aggregates or agglomerates of primary particles. It is usually clear in which way the word is being used from the context in which it is used.<sup>83,94,146–148</sup> See the [Incipient Soot Particle](#), [Aggregation and Aggregates](#), and [Agglomeration and Agglomerates](#) sections.

**Liquid-like Particles.** A liquid is a material that flows and is compliant and whose shape responds to forces such as that of gravity or surface tension. These characteristics allow a liquid to conform to the shape of its container.<sup>104,149</sup> Liquid-like particles would generally be nearly spherical as defined by surface tension. This term was coined to denote nanosized particles that exhibit certain behaviors of a bulk liquid substance. Examples include the flattening of surface-collected particles with surface morphology resembling that of wax splashing on a surface.<sup>6</sup> On average, liquids are amorphous and do not possess structural regularity or order.<sup>104</sup> Experimental investigations of incipient particles have suggested that these particles may be liquid-like at elevated temperatures.<sup>2–8</sup>

**Particle Growth. Coagulation.** Coagulation refers to the different processes that join particles together, including coalescence, aggregation, and agglomeration;<sup>14,18,94,95,110,150</sup> see the [Coalescence](#), [Aggregation and Aggregates](#), and [Agglomeration and Agglomerates](#) sections.

**Coalescence.** Coalescence is the merging of two or more particles into one in a way that removes any boundary between them. This term generally refers to particles of miscible

substances, such as water droplets or air bubbles. With respect to soot, however, it is used to describe the growth of liquid-like incipient particles through collisions that merge these particles.<sup>14,16,113,150–154</sup> Coalescence is a possible outcome of coagulation. “Sintering” has also been used to describe the coalescence of liquid-like incipient particles.<sup>155</sup> Because of the inconsistent usage of “sintering” in the soot literature, we recommend avoiding its use in this context. In addition, using “coalescence”, rather than “sintering”, allows for greater consistency and connection with the large body of literature on this topic; see the [Sintering](#) section.

**Surface Growth.** Surface growth describes the process by which gas-phase species are added to the surface to increase the mass of a soot particle. Surface growth can occur at any stage of maturity by processes including condensation, deposition, physisorption, and chemisorption, any of which can generally be referred to as “adsorption”; see the [Adsorption and Desorption](#), [Chemisorption](#), [Physisorption](#), [Condensation](#), and [Deposition](#) sections.

**Condensation.** Condensation is the thermodynamic phase transition of a gas to a liquid and is the reverse of vaporization.<sup>62–66</sup> In soot science, “condensation” has been used in the past to represent a heterogeneous gas-to-particle conversion without regard to the state of the condensed phase.<sup>14,58,98,148,156–158</sup> However, using “condensation” to describe any gas-to-particle conversion is inconsistent with the common usage in other fields, including physics, chemistry, and atmospheric and aerosol science, and it is recommended that this terminology no longer be used in describing soot processes other than when discussing the thermodynamic phase transition to produce a liquid phase by physical condensation of gaseous components. We recommend using “deposition” to represent a gas-to-solid phase transition and “adsorption” to describe interfacial uptake of material that is not the result of a thermodynamic phase transition. If the binding mechanism is known, “chemisorption” or “physisorption” may be used; see the [Deposition](#), [Adsorption and Desorption](#), [Chemisorption](#), [Physisorption](#), and [Vaporization](#), [Evaporation](#), and [Boiling](#) sections.

**Vaporization, Evaporation, and Boiling.** Vaporization is the thermodynamic phase transition of a liquid to a gas and is the reverse of condensation.<sup>62–66</sup> Evaporation is the vaporization process that occurs when the vapor pressure of the substance is lower than its saturation pressure at that temperature.<sup>159</sup> Evaporation takes place at the gas–liquid interface.<sup>159</sup> Boiling is the vaporization process that occurs at temperatures at or above the boiling point at a particular pressure;<sup>159</sup> see the [Condensation](#) section.

**Deposition.** Deposition is the thermodynamic phase transition of a gas directly into a solid and is the reverse of sublimation.<sup>63–66,160</sup> Deposition can proceed by formation of electrostatic, covalent, or metallic bonds, depending on the material. When the uptake of material onto a solid surface is not the result of a thermodynamic phase transition, “adsorption” should be used to describe the process. If the adsorption binding mechanism is known, “chemisorption” or “physisorption” may be used; see the [Sublimation](#), [Adsorption and Desorption](#), [Chemisorption](#), and [Physisorption](#) sections.

**Sublimation.** Sublimation is the thermodynamic phase transition of a solid directly into a gas and is the reverse of deposition;<sup>63–66,160</sup> see the [Deposition](#) section.

**Physisorption.** Physisorption or physical adsorption is the binding of atoms or molecules directly to a surface *via*

dispersion or van der Waals forces.<sup>102,161</sup> This term describes the physical binding mechanism and is generally used for monolayer or submonolayer interactions; these characteristics make it distinguishable from the thermodynamic phase transitions of condensation and deposition. Binding energies (energies of adsorption) are usually small, that is, in the range of 0.1–80 kJ/mol.<sup>102,162,163</sup> For a PAH physisorbed to graphite, graphene, carbon nanotubes, or soot, binding energies are on the order of 2.5–6 kJ/mol per carbon atom.<sup>164–167</sup> Such bound states are generally only stable at low temperatures<sup>162</sup> and are transient or short-lived at elevated temperatures,<sup>168</sup> where desorption becomes significant. The enthalpy of physisorption is of the same order of magnitude as the enthalpy of condensation.<sup>102</sup>

**Chemisorption.** Chemisorption or chemical adsorption is the binding of atoms or molecules directly to a surface through surface chemical bonds, that is, *via* covalent bonds.<sup>102,161,169</sup> This term describes the molecule–surface binding mechanism and is generally used for monolayer or submonolayer interactions. Chemisorption is thus distinguishable from the thermodynamic phase-transition processes of condensation and deposition. Chemisorption can occur at gas–liquid,<sup>170,171</sup> gas–solid,<sup>169,172–174</sup> or liquid–solid interfaces.<sup>174–176</sup> As with other chemical reactions, reaching a state in which the molecules or atoms are chemisorbed to a surface may involve overcoming a reaction barrier to adsorption.<sup>161,173,177</sup> Sequential chemisorption can lead to multilayer growth of new material at a surface.<sup>175</sup> Chemisorption binding energies (energies of adsorption) are on the order of 100–400 kJ/mol,<sup>102,163,178,179</sup> that is, orders of magnitude larger than physisorption binding energies. Chemisorbed species may be relatively stable at moderate flame temperatures. The rate of desorption of chemisorbed molecules may become significant at higher temperatures, depending on the binding energy and possible reaction barrier to desorption.

**Adsorption and Desorption.** “Adsorption” refers to the binding of atomic or molecular species to a solid or liquid surface by any mechanism and can lead to submonolayer, monolayer, or multilayer coatings.<sup>172,180</sup> The reverse of adsorption is desorption.<sup>102</sup>

**Chemical Evolution. Graphitization.** Graphitization is a process by which the graphitic crystallite fine structure of a carbonaceous material increases in long-range order within, and perpendicular to, the aromatic layers.<sup>14,181–184</sup> The ratio of carbon sp<sup>2</sup>-to-sp<sup>3</sup> bond hybridization increases with the size of the crystallite-layer planes, while the interlayer spacing decreases to approach that of graphite.<sup>113,141,183–187</sup> Graphitization involves the scavenging of interstitial carbon atoms from between layer planes, lateral crystallite growth, and bond rearrangement.<sup>183,188</sup> Some carbonaceous materials, including some forms of turbostratic graphite, are nongraphitizing, that is, they cannot undergo full graphitization to the most ordered form of graphite.<sup>181–184,186,187,189,190</sup>

**Carbonization.** Carbonization is the pyrolytic conversion of hydrocarbon species and substituted hydrocarbons toward elemental carbon (*i.e.*, pure carbon). It is marked by an increase in the carbon-to-hydrogen (C/H) ratio. Carbonization occurs by dehydrogenation, functional-group elimination, and molecular rearrangement.<sup>2,18,191</sup> Carbonization is generally accompanied by graphitization.<sup>8,112,186,187,192</sup> Some carbonaceous materials, known as nongraphitizing materials, cannot fully graphitize;<sup>181–184,186,187,189,190</sup> see the Graphitization section.

**Annealing.** Annealing is usually a thermally induced reactive process. During thermal annealing, a material is heated to a high temperature, held at that temperature for some time, and slowly cooled so that it reaches an equilibrium phase, or a low-energy structure, at the temperature to which it is cooled.<sup>193,194</sup> For metals, thermal annealing generally entails diffusion of atoms displaced from the lattice and defect annihilation through recombination at vacancy sites.<sup>195,196</sup> Annealing in carbon materials is proposed to occur *via* two mechanisms: (1) migration of displaced carbon atoms caught between graphitic layer planes and Frenkel defect annihilation at vacancy sites,<sup>197–199</sup> or (2) higher-barrier carbon-network rearrangements and growth, vacancy migration and clustering within layer planes or fullerene structures, and Schottky defect annihilation at crystalline edge sites.<sup>188,197</sup>

**Soot Aging.** Soot aging during combustion is the process of particle evolution from incipient soot particles toward mature soot particles.<sup>22,28,113</sup> Historically, this term was initially used to describe decreased reactivity of the surface as the particle evolves at high temperature.<sup>58</sup> In general, aging involves carbonization, graphitization, and, in most cases, particle coagulation and growth. As a result, the carbon-to-hydrogen (C/H) ratio increases;<sup>22,55,113,148,200,201</sup> the long-range carbon-lattice fine structure increases;<sup>22,201</sup> the density increases;<sup>202–204</sup> the solubility in organic solvents decreases;<sup>205,206</sup> and both the absorption cross section and emissivity increase dramatically at longer wavelengths.<sup>22,200,201,207,208</sup> In addition, property changes of the primary particles influence whether particles coalesce or agglomerate during coagulation. Liquid-like incipient particles may coalesce.<sup>14,16,113,150–154</sup> As these particles age, coalescence becomes impossible, and particles agglomerate instead of coalescing. Further aging is associated with graphitic surface growth that leads to the transition of agglomerates into aggregates.<sup>138,209</sup> Some soot models include terms that allow for a reduction in surface reactivity (controlling surface growth) as a result of surface aging at high temperatures where HACA is the predominant surface-growth mechanism.<sup>58,85,210–215</sup> It is unknown whether surface aging proceeds by the same process as that leading to aging of the bulk particle. Experimental and modeling results have suggested that, for at least some conditions (*e.g.*, at lower temperature), the bulk particle may mature more rapidly than the surface because of addition of new material to the surface, which prevents the surface from maturing.<sup>22,214</sup> In atmospheric science, particle aging involves surface reactions, coagulation with other particles, and adsorption of coatings. All of these processes can influence chemical, optical, and physical (*e.g.*, size and morphology) properties.<sup>216,217</sup> Some studies refer to aspects of the aging process as “sintering” of the carbonaceous material within primary particles,<sup>218,219</sup> but the chemical mechanisms that lead to soot aging are very different from the processes that cause sintering of other materials.<sup>220,221</sup> We thus recommend avoiding the use of “sintering” in this context. See the Coalescence, Agglomeration and Agglomerates, Aggregation and Aggregates, and Sintering sections.

**Maturity and Maturity Level.** The definition of the term “maturity” is the “quality or state of being mature or fully developed”<sup>222</sup>. Hence the maturity level of a soot particle describes how much it has evolved from inception toward a fully mature graphite-like particle.<sup>20,22,84,204,223–232</sup> The surface of the particle can have a different maturity level from that of the bulk.<sup>22,225,226</sup>

**Young Soot Particles.** Young soot particles are those in an early stage of development between inception and full maturity.<sup>19,34,52,55,113,148,186,187,200,201,207,208,227</sup>

**Partially Matured Soot Particles and Partially Graphitized Soot Particles.** Partially matured or partially graphitized soot particles have undergone some high-temperature aging but have not reached full maturity. These partially graphitized particles are in an intermediate stage between inception and maturity.<sup>191,228</sup> This expression may refer to (1) incompletely carbonized particles undergoing finite-rate carbonization<sup>20</sup> or (2) inhomogeneous particles containing completely carbonized and noncarbonized material.<sup>233–236</sup> An example of the second type of particle is one whose bulk has been carbonized but whose surface is undergoing rapid growth by hydrocarbon adsorption or deposition.<sup>22</sup> This type of particle may be more prevalent in turbulent environments, where intermixing of mature soot particles and precursors occurs, and in wildfire and exhaust plumes in which particles are cooled in the presence of semivolatile gas-phase byproducts.<sup>233,237</sup>

**Mature Soot Particles.** Mature soot particles are particles that have fully evolved at high temperature. Such particles are refractory and can be heated to the sublimation point of graphite (~4000 K),<sup>226,228,238</sup> are insoluble in polar and nonpolar solvents,<sup>226,238</sup> have a molar carbon-to-hydrogen (C/H) ratio ranging from ~8 to ~20,<sup>90,223,224,227,230</sup> and absorb strongly over a broad wavelength range from ultraviolet (UV) to infrared (IR).<sup>226</sup> These characteristics are predominantly defined by the particle's fine structure, which is described as being polycrystalline turbostratic graphite with coherent domains (crystallite regions without major defects or dislocations) slightly larger than 1 nm in diameter and 4–5 layers in thickness with an interlayer spacing of 0.34–0.35 nm.<sup>20,22,84,113,138,141,186,226,229,231,232,239–241</sup> Mature soot particles also tend to be strongly bound into ramiform aggregates of monodisperse primary particles.<sup>132,242–245</sup> For combustion conditions near the sooting threshold, however, primary particle monomers with diameters as small as 2–3 nm and optical properties consistent with mature soot have been observed.<sup>246–250</sup> Similar observations have been made of primary particle monomers with very ordered crystalline fine structure and diameters of ~5 nm in a coflow diffusion flame.<sup>251</sup> There has been one suggestion to refer to mature soot particles as "nano-sphere soot".<sup>252</sup> However, this term could be confused with synthesized "carbon nanoparticles" or "nano-organic carbon particles", and we suggest its use be avoided; see the *Nano-Organic Carbon Particles* and *Carbon Nanoparticles* sections.

**Fine Structure.** In the context of the material characteristics of soot, "fine structure" is used to refer to the internal structure or crystalline organization of the particle.<sup>242,253</sup> It is sometimes also referred to as "nanostructure".<sup>21,112,139,145,254–256</sup>

**Basic Structural Unit.** The basic structural unit (BSU) of a crystalline material is the unit cell, the smallest repeated substructure in the periodic atomic arrangement. Mature soot particles consist of material often described as polycrystalline turbostratic graphite, which is not a single-crystal material with a well-defined unit cell. The BSU for mature or partially mature soot is generally considered to be defined by the coherent domains or crystallites. In mature soot the BSU is usually 4–5 layers of graphene that are slightly larger than 1 nm in diameter with an interlayer spacing of 0.34–0.35 nm.<sup>113,138,141,183,186,201,239,241,257</sup>

**Dispersion Exponent.** The dispersion exponent is a variable that accounts for the wavelength dependence of the absorption cross section and emissivity of soot particles in the visible and near-IR spectral regions; see the *Black-Body Radiation* section. The dispersion exponent is a continuously variable function that is anticorrelated with the soot maturity level. Mature soot has a dispersion exponent of ~1, including values less than one whereas the value for young soot in flames has been measured to be as high as ~5.<sup>22,99,225,258–267</sup> Atmospheric scientists usually refer to the dispersion exponent as the "Ångström exponent" or "Ångström coefficient"; see the *Ångström Exponent* section.

**Black-Body Radiation.** An object that absorbs all photons that strike it, independently of wavelength, is known as a "black body".<sup>102</sup> The radiation emitted from such an object follows the temperature-dependent Planck function with an emissivity of one. The absorption cross section and emissivity are related by the principle of detailed balance, as given by Kirchhoff's law.<sup>268</sup> A gray body is an object that has an absorption cross section that is independent of wavelength, but, unlike a black body, a gray body does not absorb all photons that impinge on it. Gray-body radiation follows a Planck function with a constant emissivity that is <1.<sup>269</sup> Very few objects are true black or gray bodies, including soot, even when mature. In the visible and near-IR spectral regions, the emissivity of soot is approximately inversely proportional to the wavelength raised to the dispersion (or Ångström) exponent.<sup>270–272</sup> Incipient particles tend to absorb in the UV region of the spectrum but are nearly transparent in the visible and near-IR and are far from black or gray bodies.<sup>9–13</sup> As the particles mature, carbonize, and graphitize, their absorption cross sections and emissivity increase and broaden substantially. Mature soot particles absorb and emit at wavelengths in the UV, visible, and IR spectral regions, and their radiative emission is sometimes referred to as "quasi-black-body radiation" or "pseudo-black-body radiation".<sup>20,226,273–278</sup>

**Relevant Forms of Carbon. Amorphous Carbon.** Amorphous carbon (a-C) and hydrogenated amorphous carbon (a-C:H) are materials characterized by some short-range order but no long-range order (*i.e.*, the  $\pi$  electrons are largely localized) and a mixture of  $sp^2$  and  $sp^3$  hybridization.<sup>279–281</sup> Both a-C and a-C:H are semiconductors. Whereas a-C is composed of predominantly  $sp^2$ -hybridized carbon, a-C:H is largely  $sp^3$  hybridized.<sup>279</sup> High-resolution transmission electron microscopy, X-ray diffraction, and Raman spectroscopy measurements suggest that the structure of incipient or young soot particles can be described as amorphous or hydrogenated amorphous carbon.<sup>49,113,186,187,192</sup> This description is consistent with particles composed of aromatic species or a mixture of aromatic and aliphatic content.

**Graphene.** Graphene is a single layer of carbon atoms arranged in a hexagonal lattice, that is, a honeycomb structure of six-membered rings.<sup>282</sup> Each carbon atom is covalently bound to three other carbon atoms, and all bonds are  $sp^2$  hybridized.

**Graphite.** Graphite is a crystalline form of carbon in which layers of graphene are stacked. The graphene layers are aligned relative to one another in an alternating pattern, such that half of the carbon atoms in one layer align with carbon atoms in the adjacent layers, and the other half of the carbon atoms in that layer align with the centers of the hexagonal rings of the adjacent layers.<sup>280,283</sup>

**Turbostratic Graphite.** Turbostratic graphite is graphite in which the stacking of the graphene layers is uncorrelated or random.<sup>184,280,283</sup> It is sometimes referred to as “non-graphitic carbon”.<sup>189,190</sup> Some forms of turbostratic graphite can be graphitized at high temperature ( $>\sim 2000$  K), and some cannot.<sup>190</sup> The interlayer spacing for turbostratic graphite is 0.3440 nm, whereas that of graphite is 0.33539 nm.<sup>280</sup>

**Polycrystalline Graphite.** Polycrystalline graphite describes a material composed of multiple crystallites of graphite, which may or may not be aligned relative to one another.<sup>183,283</sup>

**Glassy Carbon.** Glassy carbon is a chemically inert nongraphitic and nongraphitizable form of disordered,  $sp^2$ -hybridized carbon with low porosity, high thermal stability, and low density.<sup>284–287</sup>

**Diamond.** Diamond is a crystalline form of carbon arranged in a lattice in which each carbon atom is covalently bound to four other carbon atoms in a tetrahedral structure. All bonds are  $sp^3$  hybridized. Diamond is not naturally formed at atmospheric pressure, but it can be formed at very high pressures and is observed to form during the detonation of carbon-rich explosives.<sup>288–291</sup>

**Fullerenes.** Fullerenes are composed of curved sheets of predominantly five-membered and six-membered rings of carbon that form enclosed structures.<sup>280</sup> The most well-known and stable of these structures is buckminsterfullerene, which is a sphere of 60 carbon atoms in the design of a soccer ball or European football.<sup>292</sup> Fullerenes are formed during combustion under rare conditions,<sup>293,294</sup> particularly at high temperatures,<sup>293,295</sup> low pressures,<sup>293</sup> and long residence times.<sup>296</sup>

**Carbon Onions.** Carbon onions are nested fullerenes that can be formed during the annealing of soot particles at high temperatures,<sup>297–300</sup> by electron bombardment of soot at moderate temperatures,<sup>198,301</sup> or during the detonation of carbon-rich explosives.<sup>289</sup> The center can be as small as buckminsterfullerene (0.71 nm in diameter) with an interlayer spacing of 0.33–0.34 nm, such that a carbon onion with four shells can be as small as 2.72–2.88 nm.<sup>301,302</sup> Such a particle, composed of nested icosahedral fullerenes, that is,  $C_{60}@C_{240}@C_{540}@C_{960}$ ,<sup>302</sup> would have 1800 carbon atoms.

**Carbon Nanotubes.** Carbon nanotubes are elongated fullerenes.<sup>280</sup> They can be single-walled, that is, an elongated version of  $C_{60}$ , or multiwalled, that is, an elongated version of carbon onions.

**Transition to Aggregates. Primary Particles.** In combustion science, primary particles are the subunits, that is, the elementary building blocks, of soot aggregates.<sup>14,19,303</sup> Primary particles are sometimes referred to as “monomers”.<sup>304</sup> This expression is used differently in atmospheric science, where “primary particles” refers to solid or liquid particles emitted directly into the atmosphere.<sup>92,305,306</sup> In atmospheric science, primary particles are distinguished from secondary particles, which are produced in the atmosphere from gas-phase emissions.<sup>92,305</sup> In combustion science, an aggregate or agglomerate may be considered to be a secondary particle, but “secondary particle” is not generally used to refer to an aggregate or agglomerate.

**Agglomeration and Agglomerates.** Agglomerates are groups of particles loosely held together, and agglomeration is the process that forms them.<sup>20,92,197,307,308</sup> Such particles are also known as flocculates.<sup>92</sup> With respect to soot, “agglomerates” refers to multiple primary particles loosely attached to one another. It may also be used to refer to loosely held

collections of multiple aggregates. The forces that hold agglomerates together depend on the types of particles and associated agglomeration processes. For soot, agglomeration mechanisms are unknown, but the forces are likely electrostatic forces, such as van der Waals forces; see the *van der Waals Interactions and Dispersion Forces* section. Agglomeration of primary particles occurs prior to aggregation.

**Aggregation and Aggregates.** Aggregates are particles composed of two or more smaller particles firmly bound together.<sup>20,92,197,307,308</sup> Aggregates cannot easily be broken apart, in contrast to agglomerates, which are only loosely held together. Mature soot particles are formed as aggregates of primary particles by the growth of layers of graphene on the surface of agglomerates of primary particles.<sup>138,209</sup>

**Super-Aggregates.** The term “super-aggregates” has been used to describe very large aggregates whose diameters are on the order of 2–100  $\mu\text{m}$ .<sup>309–316</sup> These particles have been observed in flames for conditions under which the soot concentration is very large<sup>309–312</sup> or the residence times are much longer than typically encountered in the laboratory or in technical combustors, such as those in inverted flames,<sup>315,316</sup> wildfires,<sup>314</sup> and large pool fires of several meters in diameter and length.<sup>309,313</sup> The mechanisms controlling their formation are less well investigated than for smaller soot aggregates, but they are hypothesized to be formed by diffusion-controlled agglomeration of aggregates.<sup>309–312,315,316</sup>

**Dendritic.** “Dendritic” means branched and is used to describe the branched-chain fractal-like morphology of mature soot particles.<sup>20,22,225,238,317–320</sup>

**Ramiform and Ramified.** “Ramiform” and “ramified” are synonymous with “dendritic” and are used to describe the branched-chain fractal-like morphology of mature soot particles.<sup>73,321–327</sup>

**Morphology.** With respect to soot, “morphology” usually refers to the size and shape of the aggregate.<sup>242</sup> This term may also refer to the size and spherical or nonspherical shape of the primary particles. “Structural morphology” is sometimes used to represent the fine structure of the particle,<sup>328</sup> but we suggest using “fine structure”, “internal structure”, “crystalline structure”, or “nanostructure” for such phenomena to avoid confusion.

**Fractal Dimension.** The fractal dimension (or Hausdorff dimension)<sup>147,329,330</sup> of a soot particle is a parameter used to characterize the morphology of the dendritic agglomerate or aggregate. Based on the mathematical description of fractal structures, the morphology of a fractal aggregate is scale invariant, that is, aggregates appear to have the same structure over multiple size scales.<sup>147,331</sup> Typical values for uncoated mature-soot particles freshly emitted from the combustor are in the range of 1.7–1.9.<sup>147,243,329–336</sup> For perspective, a straight line has a fractal dimension of 1, and a sphere has a fractal dimension of 3. Determining the fractal dimension of a soot particle is often complicated and is usually accomplished by inspecting transmission electron microscopy images of particles collected on a two-dimensional substrate<sup>147,329,330,335–339</sup> or analyzing light-scattering measurements.<sup>331,335</sup> It has also been shown that, with appropriate corrections for the flow conditions in the electrostatic classifier,<sup>304</sup> the fractal dimension can be derived by combining particle-mass and electric-mobility measurements;<sup>336</sup> normally such measurements are used to derive a related parameter known as the “mass-mobility exponent”<sup>219,304,340–345</sup> or “mass-fractal dimension”<sup>346–349</sup>.

**Restructuring.** Restructuring refers to a change of the morphology of a particle. With respect to soot, this term usually applies to the collapse of an aggregate from a dendritic structure with a fractal dimension of  $\sim 1.8$  to a compact structure with a fractal dimension  $> 2$ .<sup>180,317,336,341,346,349–357</sup> Restructuring usually occurs when the particles are coated with adsorbates prone to hydrogen bonding, which typically happens as the aggregates age in the atmosphere or cool in a tailpipe or exhaust plume.

**Sintering.** In materials science, sintering refers to the bonding and coalescence of particles into a larger cohesive structure at high temperature by mass-transport mechanisms including flow of material following melting, surface diffusion, and grain-boundary diffusion. Such processes are not likely to occur with mature, carbonized, and aggregated particles because these particles are composed of covalently bound graphite crystallites that do not melt or readily migrate.<sup>358</sup> Some studies have described the evolution of the soot fine structure during soot aging as “sintering” of the primary particles,<sup>218,219</sup> but we recommend referring to these processes as “soot aging”. One study presented experimental evidence for a reduction in surface area of soot aggregates during pyrolysis, which the authors referred to as “sintering”,<sup>359</sup> but the evidence presented in this paper is consistent with aggregate restructuring and is unlikely to be attributable to a sintering process. “Sintering” has also been used to describe the coalescence of liquid-like incipient particles.<sup>155</sup> Because of the inconsistent usage and resulting confusion associated with “sintering”, we recommend the use of “coalescence” to describe this process, which is consistent with the vast body of literature on this topic; see the *Soot Aging, Restructuring, and Coalescence* sections.

**Oxidation and Breakup.** **Oxidation.** With respect to soot, “oxidation” usually refers to the reaction of O<sub>3</sub>, O<sub>2</sub>, O, or OH with the particle to form CO, CO<sub>2</sub>, and H<sub>2</sub>O.<sup>360–363</sup> Oxidation reduces soot mass by converting the solid-phase particle to gas-phase products. At elevated temperatures, soot can also be oxidized by other oxygen-containing species, such as CO<sub>2</sub> to form 2CO or H<sub>2</sub>O to form CO and H<sub>2</sub>.<sup>364</sup>

**Fragmentation.** With respect to oxidation of soot particles, “fragmentation” refers to the process of the breaking-up of the particles into smaller particles.<sup>361,365–367</sup> As overlayers of graphene are oxidized, connections between primary particles are weakened, which can cause aggregates to break apart at the interface between primary particles. In addition, primary particles may also break apart.<sup>365,367</sup> Fragmentation of primary particles is hypothesized to occur *via* oxygen diffusion into the bulk of the primary particles.<sup>361,365</sup>

**Associated Expressions.** **Black Carbon.** Mature soot particles that are emitted into the atmosphere fall into a category of strongly absorbing atmospheric particles called “black carbon (BC)” or “black carbon particles”.<sup>238,368–372</sup> Mature soot particles represent the vast majority of atmospheric BC. Previous reviews of atmospheric particles have suggested that “BC” be used to refer strictly to mature soot particles.<sup>369</sup> The proposed definition specifically recommends that BC particles are formed during combustion or pyrolysis and have the following characteristics: strong absorption in the visible spectral region, sublimation temperature of  $\sim 4000$  K, graphitic fine structure, morphology of aggregated spheres, and lack of solubility in polar and nonpolar solvents.<sup>369,372</sup> Such particles are often measured using LII and

are referred to as “refractory black carbon”;<sup>369,370</sup> see the *Mature Soot Particles* section.

**Brown Carbon.** Brown carbon (BrC) is a broad category of atmospheric particles that includes young soot particles emitted into the atmosphere. These particles absorb less strongly and broadly than BC,<sup>369,373</sup> and they are usually soluble in some organic solvents.<sup>369,373,374</sup> Compared to BC, their absorption spectrum is enhanced at short visible wavelengths relative to longer wavelengths, making them appear brown rather than black.<sup>238,373</sup> Brown-carbon particles are consistently observed in association with biomass or biofuel burning and may be emitted directly into the atmosphere from such sources.<sup>236</sup> They can be produced as secondary organic aerosols by condensation of semivolatile or nonvolatile hydrocarbons often emitted into the atmosphere during incomplete combustion or pyrolysis, such as from smoldering fires or from biogenic sources.<sup>233,236,375</sup> They may also be composed of humic-like substances from soil.<sup>233,236</sup>

**Elemental Carbon.** “Elemental carbon” is an expression used by the atmospheric science community to describe particles that are emitted by combustion sources<sup>376</sup> and are extremely high in carbon relative to other elements,<sup>372</sup> are refractory and can be heated to the sublimation point of graphite ( $\sim 4000$  K), and are resistant to oxidation at temperatures below 340 °C.<sup>370,377</sup> In combustion science, such particles are referred to as “mature soot particles”; see the *Mature Soot Particles* section.

**Organic Carbon.** “Organic carbon” describes atmospheric particles composed of carbon combined with hydrogen, oxygen, nitrogen, sulfur, and/or other elements.<sup>372</sup> Most of these particles absorb strongly in the IR and UV but are nearly transparent in the visible and near-IR spectral regions.<sup>236</sup> Some of them, however, absorb in the visible and UV regions and are referred to as “BrC particles”. Incipient soot particles and young soot particles are included in this category of atmospheric particles; see the *Brown Carbon* section.

**Ångström Exponent.** The Ångström exponent or coefficient is a variable used to express the wavelength dependence of the absorption cross section and emissivity of black and brown carbon in the visible and near-IR regions of the spectrum.<sup>373,378–380</sup> It is sometimes referred to as the “absorption Ångström exponent” or “absorption Ångström coefficient”. An Ångström exponent close to 1 is associated with BC, whereas BrC has an Ångström exponent that can be considerably larger than 1.<sup>373,378–384</sup> In combustion science, the Ångström exponent is generally referred to as the “dispersion exponent”; it is continuously variable and anticorrelated with soot maturity level. Although the Ångström exponent is continuously variable between values associated with BC and BrC, the value at which BC is distinguished from BrC is not precisely defined.<sup>373,380</sup> In addition, the adsorption or attachment of non-absorbing material to BC particles (*i.e.*, *via* internal mixing) can increase the Ångström exponent,<sup>378–380,383–385</sup> and mixtures of coarse and fine particles may further influence its value.<sup>383,386</sup> See the *Black-Body Radiation and Dispersion Exponent* sections.

**Carbon Black.** Carbon black represents a wide variety of engineered forms of mature soot.<sup>73,242,387</sup>

**Carbon Nanoparticles.** The expression “carbon nanoparticles” is usually used to represent deliberately synthesized nanometer-scaled carbonaceous particles, including fullerenes, single- and multiwalled carbon nanotubes, and quantum dots.<sup>382,388–392</sup>

**Aerosol.** An aerosol is an ensemble of liquid and/or solid particles suspended in a gaseous medium,<sup>92,305</sup> whereas an aerosol particle is a single particle in an ensemble of suspended particles.<sup>305</sup>

**Smoke.** Smoke is a suspension of combustion-generated particles that is concentrated enough to be visible to the naked eye.<sup>393</sup> These particles are usually mature or nearly mature soot particles, but may include less mature soot particles that have coagulated or are coated with semivolatile combustion byproducts. Smoke can also include emissions of condensed unburned fuel, partially oxidized fuel species, charred fuel fragments, water droplets, and other coemitted byproducts of combustion.<sup>394,395</sup>

**Smoke Number.** The smoke number is a metric developed to assess qualitatively the production of soot emissions from jet engines and other combustors.<sup>396</sup> The original purpose of the smoke number was to minimize visibility of the smoke plume from aircraft engines. Smoke number represents the fractional reduction in reflectance by a smoke filter due to the blackening of its surface by soot contained in exhaust gases. This standard is being replaced by new criteria on soot-mass and particle-number emissions.<sup>396</sup>

**Smoke Point.** Measurement of the smoke point (SP) is a standardized test method to estimate the propensity of kerosene or an aviation jet fuel to produce soot emissions in a combustor (ASTM D1322).<sup>397</sup> A wick flame is created using the test fuel, and the SP is the height above the wick at which visible soot is first observed by eye. Hence, fuels with higher SPs have a lower propensity to produce soot. “Smoke point” can also refer to the burning point, that is, the temperature at which a heated oil or fat begins to continuously produce a visible bluish “smoke” plume. See the *Threshold Sooting Index* and *Yield Sooting Index* sections.

**Sooting Threshold.** The sooting threshold is generally identified for burner-stabilized premixed flames as the smallest equivalence ratio, or carbon-to-oxygen (C/O) ratio, at which soot luminescence is observable.<sup>84,398–400</sup> The sooting threshold has typically been determined by observations of the onset of visible soot luminosity<sup>400–404</sup> or visible light absorption<sup>13</sup> as the fuel, fuel-to-oxidizer ratio, or some other parameter is varied. As noted previously,<sup>84,405</sup> this expression is an example of an imprecise operational term that depends on how the soot onset is observed and interpreted.

**Threshold Sooting Index.** The threshold sooting index (TSI) is a standard of measurement developed in the 1980s<sup>406</sup> to rank the propensity of various hydrocarbon fuels to produce soot. The method uses the SP configuration but reduces the subjectivity of assessments by eye in the SP tests. The technique was subsequently extended to complex surrogates and heavily sooting fuels.<sup>397,407</sup> The TSI can be related to the SP via the molecular weight (MW) of the fuel:  $TSI = a(MW/SP) + b$ , where  $a$  and  $b$  are apparatus-specific empirical parameters.<sup>408,409</sup> See also the *Smoke Point* and *Yield Sooting Index* sections.

**Yield Sooting Index.** Yield sooting index (YSI) was introduced in 2007 as an improvement over TSI using a much more accurate technique than the SP (*i.e.*, LII) to measure soot volume fraction.<sup>410</sup> Although LII is frequently used to measure volume fraction for YSI,<sup>409–413</sup> laser extinction<sup>414,415</sup> and color ratio pyrometry<sup>416,417</sup> are also used with the assumption of the optical properties of mature soot particles. YSI is measured on an experimental configuration different from that for the SP and TSI for

determination of the propensity of a given fuel to produce soot. The measurement of YSI uses a well-established coflow nonpremixed methane flame with a defined thermal profile to which small amounts of a selected fuel are added. The soot volume fraction ( $f_v$ ) is measured on the flame axis if LII is used, along the line-of-sight if extinction is used, or radially integrated if spatially resolved color ratio pyrometry is used.<sup>409–413,416,417</sup> YSI is calculated according to  $YSI = Af_{v,\max} + B$ , where  $f_{v,\max}$  is the maximum in  $f_v$  with respect to height in the flame, which is usually along the flame axis for the low-sooting methane flames typically used. The empirical apparatus-specific constants,  $A$  and  $B$ , are chosen to give a value for YSI of 0 for *n*-hexane and 100 for benzene.<sup>409–413,416,417</sup> YSI has been found to be more accurate than the SP and TSI for aircraft fuels and has been applied to diesel fuels as well. See also the *Smoke Point* and *Threshold Sooting Index* sections.

**Nonvolatile Particulate Matter and Volatile Particulate Matter.** Nonvolatile particulate matter (nvPM) is a term used by the aircraft industry and others to represent the component of particles that are not volatile below 350 °C.<sup>418,419</sup> Volatile components, that is, volatile particulate matter (vPM), include H<sub>2</sub>SO<sub>4</sub>, water, unburned fuel, and PAHs.<sup>419</sup> The nvPM contributions to particulate matter are solid and consist primarily of mature soot particles.<sup>306,419</sup>

## CONCLUSIONS

In this review of the terminology employed in the study of soot chemistry, properties, and modeling, we have sought to synthesize a consistent framework to describe these highly complex processes and to highlight a few terms that we suggest avoiding in order to minimize confusion. Nevertheless, the processes and transitions between one state and another are not yet well-defined and likely depend on conditions. Hence, this review may need to be expanded in the future, as the community’s understanding of soot evolves. For example, we may need to revise our description of the soot inception processes and introduce more specificity to the terminology as the understanding of the details grows beyond its presently limited status. We can also anticipate that new terms will need to be developed to describe the levels of maturity of the particles as they evolve from incipient soot particles to mature soot particles.

In addition to facilitating communication within the field of soot science, this review is meant to enable better communication between scientific communities. The last section, in particular, is a potential springboard for enhancing the understanding of the underlying physical and chemical characteristics of combustion-generated black and brown carbon particles in the atmosphere. Because there is a very poor understanding in the atmospheric community of how these particles are produced, their descriptions tend to be phenomenological rather than physically based. Enabling better communication between these communities is likely to increase the understanding of soot emissions in both communities.

Better communication between the soot science and materials synthesis communities is also potentially useful for advancing targeted carbonaceous materials production and product innovation. There are exciting developments in the production of exotic materials, such as nanodiamonds, carbon nanocones, nanodisks, nanotubes, and other nanostructures.<sup>420–430</sup> Understanding the conditions under which such

materials are produced is likely to lead to a better understanding of soot chemistry. We thus hope that the present review will serve to bring more consistency to the field of soot science, to facilitate collaborations and bridging between fields associated with the growth of carbonaceous materials at high temperature, and to aid the advancement of combustion science by highlighting gaps in our understanding of soot formation.

## AUTHOR INFORMATION

### Corresponding Author

**Hope A. Michelsen** — Rady Department of Mechanical Engineering and Environmental Engineering Program, University of Colorado Boulder, Boulder, Colorado 80309, United States;  orcid.org/0000-0001-5802-6615; Email: Hope.Michelsen@colorado.edu

### Authors

**Meredith B. Colket** — United Technologies Research Center, Avon, Connecticut 06001, United States

**Per-Erik Bengtsson** — Division of Combustion Physics, Lund University, 221 00 Lund, Sweden

**Andrea D'Anna** — Dipartimento di Ingegneria Chimica dei Materiali e della Produzione Industriale, Università degli Studi di Napoli Federico II, 80125 Napoli, Italy;  orcid.org/0000-0001-9018-3637

**Pascale Desgroux** — UMR-8522-PC2A-Physicochimie des Processus de Combustion et de l'Atmosphère, Université Lille, CNRS, F-59000 Lille, France

**Brian S. Haynes** — School of Chemical and Biomolecular Engineering, University of Sydney, Sydney, New South Wales 2006, Australia

**J. Houston Miller** — Department of Chemistry, George Washington University, Washington, D.C. 20052, United States

**Graham J. Nathan** — School of Mechanical Engineering, University of Adelaide, SA 5005 Adelaide, Australia

**Heinz Pitsch** — Institute for Combustion Technology, RWTH Aachen University, 52056 Aachen, Germany

**Hai Wang** — Department of Mechanical Engineering, Stanford University, Stanford, California 94305, United States

Complete contact information is available at:

<https://pubs.acs.org/10.1021/acsnano.0c06226>

### Notes

The authors declare no competing financial interest.

## ACKNOWLEDGMENTS

We have all benefitted from the enormous contributions from Prof. Heinz Gg. Wagner (1928–2020) who was one of the early pioneers of the field of soot formation chemistry. This paper was submitted on the 100th birthday of Dr. Rosalind Franklin. We are honored to acknowledge her with tremendous gratitude for her early contributions to this field. We are grateful to Lukas Berger, Antonio Attili, Joel Corbin, and Alex Laskin for reading the manuscript and providing thoughtful input. H.A.M. was supported by the U.S. Department of Energy, Office of Science, Office of Basic Energy Sciences, Division of Chemical Sciences, Geosciences, and Biosciences as part of the Gas-Phase Chemical Physics Program under a subcontract from Sandia National Laboratories and the College of Engineering and Applied Sciences at the University of Colorado Boulder. M.C. is indebted to both the Air Force Office of Scientific Research (AFOSR),

through Dr. Julian Tishkoff, and the Strategic Environmental Research and Development Program with team leadership by Mel Roquemore for sustained multiyear funding. J.H.M. was supported by the U.S. National Science Foundation under Grant Number CBET-1706757 with Drs. Song-Charng Kon and Harsha Chelliah serving as technical monitors. G.J.N. acknowledges support from the Australian Research Council through grant DP19010112. H.P. acknowledges support from Deutsche Forschungsgemeinschaft (DFG) and the Research Association for Combustion Engines (FVV) under grant numbers PI 368/25-1 (DFG) and 6013970 (FVV). H.W. acknowledges support from AFOSR under grant FA9550-19-1-0261.

## REFERENCES

- (1) International Sooting Flame Workshop. <https://www.adelaide.edu.au/cet/isfworkshop/2018-workshop/> (accessed 2020-09-30).
- (2) Vander Wal, R. L. Soot Precursor Carbonization: Visualization Using LIF and LII and Comparison Using Bright and Dark Field TEM. *Combust. Flame* **1998**, *112*, 607–616.
- (3) Dobbins, R. A. Hydrocarbon Nanoparticles Formed in Flames and Diesel Engines. *Aerosol Sci. Technol.* **2007**, *41*, 485–496.
- (4) Zhao, B.; Uchikawa, K.; Wang, H. A Comparative Study of Nanoparticles in Premixed Flames by Scanning Mobility Particle Sizer, Small Angle Neutron Scattering, and Transmission Electron Microscopy. *Proc. Combust. Inst.* **2007**, *31*, 851–860.
- (5) Maricq, M. M. An Examination of Soot Composition in Premixed Hydrocarbon Flames Via Laser Ablation Particle Mass Spectrometry. *J. Aerosol Sci.* **2009**, *40*, 844–857.
- (6) Abid, A. D.; Tolmachoff, E. D.; Phares, D. J.; Wang, H.; Liu, Y.; Laskin, A. Size Distribution and Morphology of Nascent Soot in Premixed Ethylene Flames with and without Benzene. *Proc. Combust. Inst.* **2009**, *32*, 681–688.
- (7) Khalghy, M. R.; Saffaripour, M.; Yip, C.; Thomson, M. J. The Evolution of Soot Morphology in a Laminar Coflow Diffusion Flame of a Surrogate for Jet A-1. *Combust. Flame* **2013**, *160*, 2119–2130.
- (8) Russo, C.; Tregrossi, A.; Ciajolo, A. Dehydrogenation and Growth of Soot in Premixed Flames. *Proc. Combust. Inst.* **2015**, *35*, 1803–1809.
- (9) D'Alessio, A.; D'Anna, A.; Gambi, G.; Minutolo, P. The Spectroscopic Characterisation of UV Absorbing Nanoparticles in Fuel Rich Soot Forming Flames. *J. Aerosol Sci.* **1998**, *29*, 397–409.
- (10) Basile, G.; Rolando, A.; D'Alessio, A.; D'Anna, A.; Minutolo, P. Coagulation and Carbonization Processes in Slightly Sooting Premixed Flames. *Proc. Combust. Inst.* **2002**, *29*, 2391–2397.
- (11) Sgro, L. A.; Basile, G.; Barone, A. C.; D'Anna, A.; Minutolo, P.; Borghese, A.; D'Alessio, A. Detection of Combustion Formed Nanoparticles. *Chemosphere* **2003**, *51*, 1079–1090.
- (12) D'Anna, A.; Rolando, A.; Allouis, C.; Minutolo, P.; D'Alessio, A. Nano-Organic Carbon and Soot Particle Measurements in a Laminar Ethylene Diffusion Flame. *Proc. Combust. Inst.* **2005**, *30*, 1449–1456.
- (13) Sgro, L. A.; Barone, A. C.; Commodo, M.; D'Alessio, A.; De Filippo, A.; Lanzuolo, G.; Minutolo, P. Measurement of Nanoparticles of Organic Carbon in Non-Sooting Flame Conditions. *Proc. Combust. Inst.* **2009**, *32*, 689–696.
- (14) Haynes, B. S.; Wagner, H. G. Soot Formation. *Prog. Energy Combust. Sci.* **1981**, *7*, 229–273.
- (15) Calcote, H. F. Mechanisms of Soot Nucleation in Flames: A Critical Review. *Combust. Flame* **1981**, *42*, 215–242.
- (16) Harris, S. J.; Weiner, A. M. Chemical Kinetics of Soot Particle Growth. *Annu. Rev. Phys. Chem.* **1985**, *36*, 31–52.
- (17) Bockhorn, H. *Soot Formation in Combustion: Mechanisms and Models*; Springer-Verlag: Berlin, 1994; Vol. 59, p 596.
- (18) Richter, H.; Howard, J. B. Formation of Polycyclic Aromatic Hydrocarbons and Their Growth to Soot: A Review of Chemical Reaction Pathways. *Prog. Energy Combust. Sci.* **2000**, *26*, 565–608.

- (19) Wang, H. Formation of Nascent Soot and Other Condensed-Phase Materials in Flames. *Proc. Combust. Inst.* **2011**, *33*, 41–67.
- (20) Michelsen, H. A. Probing Soot Formation, Chemical and Physical Evolution, and Oxidation: A Review of *In Situ* Diagnostic Techniques and Needs. *Proc. Combust. Inst.* **2017**, *36*, 717–735.
- (21) Müller, J.-O.; Su, D. S.; Wild, U.; Schlögl, R. Bulk and Surface Structural Investigations of Diesel Engine Soot and Carbon Black. *Phys. Chem. Chem. Phys.* **2007**, *9*, 4018–4025.
- (22) Johansson, K. O.; El Gabaly, F.; Schrader, P. E.; Campbell, M. F.; Michelsen, H. A. Evolution of Maturity Levels of Particle Surface and Bulk During Soot Growth and Oxidation in a Flame. *Aerosol Sci. Technol.* **2017**, *51*, 1333–1344.
- (23) Johansson, K. O.; Head-Gordon, M. P.; Schrader, P. E.; Wilson, K. R.; Michelsen, H. A. Resonance-Stabilized Hydrocarbon Radical Chain Reactions May Explain Soot Inception and Growth. *Science* **2018**, *361*, 997–1000.
- (24) Berry, R. S.; Rice, S. A.; Ross, J. *Physical Chemistry*; Wiley & Sons: New York, 1980; p 1264.
- (25) Masterton, W. L.; Slowinski, E. J. *Chemical Principles*; W. B. Saunders Company: Philadelphia, PA, 1977.
- (26) Lindstedt, P. Modeling of the Chemical Complexities of Flames. *Symp. (Int.) Combust., [Proc.]* **1998**, *27*, 269–285.
- (27) Leung, K.M.; Lindstedt, R.P.; Jones, W.P. A Simplified Reaction Mechanism for Soot Formation in Nonpremixed Flames. *Combust. Flame* **1991**, *87*, 289–305.
- (28) Kennedy, I. M. Models of Soot Formation and Oxidation. *Prog. Energy Combust. Sci.* **1997**, *23*, 95–132.
- (29) Miller, J. H.; Smyth, K. C.; Mallard, W. G. Calculations of the Dimerization of Aromatic Hydrocarbons: Implications for Soot Formation. *Symp. (Int.) Combust., [Proc.]* **1985**, *20*, 1139–1147.
- (30) Totton, T. S.; Misquitta, A. J.; Kraft, M. A Quantitative Study of the Clustering of Polycyclic Aromatic Hydrocarbons at High Temperatures. *Phys. Chem. Chem. Phys.* **2012**, *14*, 4081–4094.
- (31) Elvati, P.; Violi, A. Thermodynamics of Poly-Aromatic Hydrocarbon Clustering and the Effects of Substituted Aliphatic Chains. *Proc. Combust. Inst.* **2013**, *34*, 1837–1843.
- (32) Mercier, X.; Carrivain, O.; Irimie, C.; Faccinetto, A.; Therssen, E. Dimers of Polycyclic Aromatic Hydrocarbons: The Missing Pieces in the Soot Formation Process. *Phys. Chem. Chem. Phys.* **2019**, *21*, 8282–8294.
- (33) Chung, S.-H.; Violi, A. Peri-Condensed Aromatics with Aliphatic Chains as Key Intermediates for the Nucleation of Aromatic Hydrocarbons. *Proc. Combust. Inst.* **2011**, *33*, 693–700.
- (34) Skeen, S. A.; Michelsen, H. A.; Wilson, K. R.; Popolan, D. M.; Violi, A.; Hansen, N. Near-Threshold Photoionization Mass Spectra of Combustion-Generated High-Molecular-Weight Soot Precursors. *J. Aerosol Sci.* **2013**, *58*, 86–102.
- (35) Cain, J. P.; Laskin, A.; Khalghy, M. R.; Thomson, M. J.; Wang, H. Molecular Characterization of Organic Content of Soot Along the Centerline of a Coflow Diffusion Flame. *Phys. Chem. Chem. Phys.* **2014**, *16*, 25862–25875.
- (36) Minutolo, P.; Gambi, G.; D'Alessio, A.; Carlucci, S. Spectroscopic Characterisation of Carbonaceous Nanoparticles in Premixed Flames. *Atmos. Environ.* **1999**, *33*, 2725–2732.
- (37) Sirignano, M.; Collina, A.; Commodo, M.; Minutolo, P.; D'Anna, A. Detection of Aromatic Hydrocarbons and Incipient Particles in an Opposed-Flow Flame of Ethylene by Spectral and Time-Resolved Laser Induced Emission Spectroscopy. *Combust. Flame* **2012**, *159*, 1663–1669.
- (38) Adamson, B. D.; Skeen, S. A.; Ahmed, M.; Hansen, N. Detection of Aliphatically Bridged Multi-Core Polycyclic Aromatic Hydrocarbons in Sooting Flames with Atmospheric-Sampling High-Resolution Tandem Mass Spectrometry. *J. Phys. Chem. A* **2018**, *122*, 9338–9349.
- (39) Schulz, F.; Commodo, M.; Kaiser, K.; De Falco, G.; Minutolo, P.; Meyer, G.; D'Anna, A.; Gross, L. Insights into Incipient Soot Formation by Atomic Force Microscopy. *Proc. Combust. Inst.* **2019**, *37*, 885–892.
- (40) Commodo, M.; Kaiser, K.; De Falco, G.; Minutolo, P.; Schulz, F.; D'Anna, A.; Gross, L. On the Early Stages of Soot Formation: Molecular Structure Elucidation by High-Resolution Atomic Force Microscopy. *Combust. Flame* **2019**, *205*, 154–164.
- (41) Weilmünster, P.; Keller, A.; Homann, K.-H. Large Molecules, Radicals, Ions, and Small Soot Particles in Fuel-Rich Hydrocarbon Flames Part I: Positive Ions of Polycyclic Aromatic Hydrocarbons (PAH) in Low-Pressure Premixed Flames of Acetylene and Oxygen. *Combust. Flame* **1999**, *116*, 62–83.
- (42) Martin, J. W.; Botero, M.; Slavchov, R. I.; Bowal, K.; Akroyd, J.; Mosbach, S.; Kraft, M. Flexoelectricity and the Formation of Carbon Nanoparticles in Flames. *J. Phys. Chem. C* **2018**, *122*, 22210–22215.
- (43) Yuan, H.; Kong, W.; Liu, F.; Chen, D. Study on Soot Nucleation and Growth from PAHs and Some Reactive Species at Flame Temperatures by ReaxFF Molecular Dynamics. *Chem. Eng. Sci.* **2019**, *195*, 748–757.
- (44) Vitiello, G.; De Falco, G.; Picca, F.; Commodo, M.; D'Errico, G.; Minutolo, P.; D'Anna, A. Role of Radicals in Carbon Clustering and Soot Inception: A Combined EPR and Raman Spectroscopic Study. *Combust. Flame* **2019**, *205*, 286–294.
- (45) Rusciano, G.; De Luca, A. C.; D'Alessio, A.; Minutolo, P.; Pesce, G.; Sasso, A. Surface-Enhanced Raman Scattering Study of Nano-Sized Organic Carbon Particles Produced in Combustion Processes. *Carbon* **2008**, *46*, 335–341.
- (46) D'Anna, A. Combustion-Formed Nanoparticles. *Proc. Combust. Inst.* **2009**, *32*, 593–613.
- (47) Dobbins, R. A.; Subramanian, H. Soot Precursors: Particles in Flames. In *Soot Formation in Combustion*; Bockhorn, H., Ed.; Springer-Verlag: Berlin, 1994; pp 290–301.
- (48) D'Anna, A.; D'Alessio, A.; Minutolo, P., Spectroscopic and Chemical Characterization of Soot Inception Processes in Premixed Laminar Flames at Atmospheric Pressure. In *Soot Formation in Combustion: Mechanisms and Models*; Bockhorn, H., Ed.; Springer-Verlag: Berlin, 1994; Vol. 59, pp 83–103.
- (49) Vander Wal, R. L. Soot Precursor Material: Visualization Via Simultaneous LIF-LII and Characterization Via TEM. *Symp. (Int.) Combust., [Proc.]* **1996**, *26*, 2269–2275.
- (50) Reilly, P. T. A.; Gieray, R. A.; Whitten, W. B.; Ramsey, J. M. Direct Observation of the Evolution of the Soot Carbonization Process in an Acetylene Diffusion Flame Via Real-Time Aerosol Mass Spectrometry. *Combust. Flame* **2000**, *122*, 90–104.
- (51) Dobbins, R. A. Soot Inception Temperature and the Carbonization Rate of Precursor Particles. *Combust. Flame* **2002**, *130*, 204–214.
- (52) Blevins, L. G.; Fletcher, R. A.; Benner, B. A.; Steel, E. B.; Mulholland, G. W. The Existence of Young Soot in the Exhaust of Inverse Diffusion Flames. *Proc. Combust. Inst.* **2002**, *29*, 2325–2333.
- (53) Happold, J.; Grotheer, H.-H.; Aigner, M. Distinction of Gaseous Soot Precursor Molecules and Soot Precursor Particles through Photoionization Mass Spectrometry. *Rapid Commun. Mass Spectrom.* **2007**, *21*, 1247–1254.
- (54) Maricq, M. M. Physical and Chemical Comparison of Soot in Hydrocarbon and Biodiesel Fuel Diffusion Flames: A Study of Model and Commercial Fuels. *Combust. Flame* **2011**, *158*, 105–116.
- (55) Harris, S. J.; Weiner, A. M. Surface Growth of Soot Particles in Premixed Ethylene/Air Flames. *Combust. Sci. Technol.* **1983**, *31*, 155–167.
- (56) Haynes, B. S.; Wagner, H. G. The Surface Growth Phenomenon in Soot Formation. *Z. Phys. Chem.* **1982**, *133*, 201–213.
- (57) Frenklach, M. On Surface Growth Mechanism of Soot Particles. *Symp. (Int.) Combust., [Proc.]* **1996**, *26*, 2285–2293.
- (58) Frenklach, M.; Wang, H. Detailed Modeling of Soot Particle Nucleation and Growth. *Symp. (Int.) Combust., [Proc.]* **1991**, *23*, 1559–1566.
- (59) Howard, J. B. Carbon Addition and Oxidation Reactions in Heterogeneous Combustion and Soot Formation. *Symp. (Int.) Combust., [Proc.]* **1991**, *23*, 1107–1127.

- (60) Benish, T. G.; Lafeur, A. L.; Taghiadeh, K.; Howard, J. B. C<sub>2</sub>H<sub>2</sub> and PAH as Soot Growth Reactants in Premixed C<sub>2</sub>H<sub>4</sub>-Air Flames. *Symp. (Int.) Combust., [Proc.]* **1996**, *26*, 2319–2326.
- (61) D'Alessio, A.; D'Anna, A.; Minutolo, P.; Sgro, L. A.; Violi, A. On the Relevance of Surface Growth in Soot Formation in Premixed Flames. *Proc. Combust. Inst.* **2000**, *28*, 2547–2554.
- (62) Cernuschi, F.; Eyring, H. An Elementary Theory of Condensation. *J. Chem. Phys.* **1939**, *7*, 547–551.
- (63) McDonald, J. E. “Deposition”: A Proposed Antonym for “Sublimation”. *J. Meteorol.* **1958**, *15*, 245–247.
- (64) Jacobson, M. Z. *Fundamentals of Atmospheric Modeling*, 2nd ed.; Cambridge University Press: Cambridge, 2005.
- (65) Dymarska, M.; Murray, B. J.; Sun, L.; Eastwood, M. L.; Knopf, D. A.; Bertram, A. K. Deposition Ice Nucleation on Soot at Temperatures Relevant for the Lower Troposphere. *J. Geophys. Res.* **2006**, *111*, D04204.
- (66) Veshkini, A.; Eaves, N. A.; Dworkin, S. B.; Thomson, K. A. Application of PAH-Condensation Reversibility in Modeling Soot Growth in Laminar Premixed and Nonpremixed Flames. *Combust. Flame* **2016**, *167*, 335–352.
- (67) Bockhorn, H.; Fetting, F.; Wannemacher, G.; Wenz, H. W. Optical Studies of Soot Particle Growth in Hydrocarbon Oxygen Flames. *Symp. (Int.) Combust., [Proc.]* **1982**, *19*, 1413–1420.
- (68) Prado, G.; Lahaye, J.; Haynes, B. S. Soot Particle Nucleation and Agglomeration. In *Soot in Combustion Systems and Its Toxic Properties*; Lahaye, J.; Prado, G., Eds.; Springer: Boston, MA, 1983; Vol. 7, pp 145–161.
- (69) Smyth, K. C.; Miller, J. H.; Dorfman, R. C.; Mallard, W. G.; Santoro, R. J. Soot Inception in a Methane/Air Diffusion Flame as Characterized by Detailed Species Profiles. *Combust. Flame* **1985**, *62*, 157–181.
- (70) Harris, S. J.; Weiner, A. M.; Ashcraft, C. C. Soot Particle Inception Kinetics in a Premixed Ethylene Flame. *Combust. Flame* **1986**, *64*, 65–81.
- (71) Glassman, I. Soot Formation in Combustion Processes. *Symp. (Int.) Combust., [Proc.]* **1989**, *22*, 295–311.
- (72) McKinnon, J. T.; Howard, J. B. The Roles of PAH and Acetylene in Soot Nucleation and Growth. *Symp. (Int.) Combust., [Proc.]* **1992**, *24*, 965–971.
- (73) Lahaye, J.; Ehrburger-Dolle, F. Mechanisms of Carbon Black Formation: Correlation with the Morphology of Aggregates. *Carbon* **1994**, *32*, 1319–1324.
- (74) Colket, M. B.; Hall, R. J. Successes and Uncertainties in Modeling Soot Formation in Laminar, Premixed Flames. In *Soot Formation in Combustion: Mechanisms and Models*; Bockhorn, H., Ed.; Springer-Verlag: Berlin, 1994; pp 442–470.
- (75) Frenklach, M. Reaction Mechanism of Soot Formation in Flames. *Phys. Chem. Chem. Phys.* **2002**, *4*, 2028–2037.
- (76) Zhao, B.; Yang, Z.; Johnston, M. V.; Wang, H.; Wexler, A. S.; Balthasar, M.; Kraft, M. Measurement and Numerical Simulation of Soot Particle Size Distribution Functions in a Laminar Premixed Ethylene-Oxygen-Argon Flame. *Combust. Flame* **2003**, *133*, 173–188.
- (77) Violi, A. Modeling of Soot Particle Inception in Aromatic and Aliphatic Premixed Flames. *Combust. Flame* **2004**, *139*, 279–287.
- (78) Singh, J.; Patterson, R. I. A.; Kraft, M.; Wang, H. Numerical Simulation and Sensitivity Analysis of Detailed Soot Particle Size Distribution in Laminar Premixed Ethylene Flames. *Combust. Flame* **2006**, *145*, 117–127.
- (79) D'Anna, A.; Sirignano, M.; Kent, J. A Model of Particle Nucleation in Premixed Ethylene Flames. *Combust. Flame* **2010**, *157*, 2106–2115.
- (80) Totton, T. S.; Chakrabarti, D.; Misquitta, A. J.; Sander, M.; Wales, D. J.; Kraft, M. Modelling the Internal Structure of Nascent Soot Particles. *Combust. Flame* **2010**, *157*, 909–914.
- (81) Cain, J. P.; Gassman, P. L.; Wang, H.; Laskin, A. Micro-FTIR Study of Soot Chemical Composition - Evidence of Aliphatic Hydrocarbons on Nascent Soot Surfaces. *Phys. Chem. Chem. Phys.* **2010**, *12*, 5206–5218.
- (82) Teini, P. D.; Karwat, D. M. A.; Atreya, A. Observations of Nascent Soot: Molecular Deposition and Particle Morphology. *Combust. Flame* **2011**, *158*, 2045–2055.
- (83) Maricq, M. M. Soot Formation in Ethanol/Gasoline Fuel Blend Diffusion Flames. *Combust. Flame* **2012**, *159*, 170–180.
- (84) Desgroux, P.; Mercier, X.; Thomson, K. A. Study of the Formation of Soot and Its Precursors in Flames Using Optical Diagnostics. *Proc. Combust. Inst.* **2013**, *34*, 1713–1738.
- (85) Veshkini, A.; Dworkin, S. B.; Thomson, M. J. A Soot Particle Surface Reactivity Model Applied to a Wide Range of Laminar Ethylene/Air Flames. *Combust. Flame* **2014**, *161*, 3191–3200.
- (86) Commodo, M.; De Falco, G.; Bruno, A.; Borriello, C.; Minutolo, P.; D'Anna, A. Physicochemical Evolution of Nascent Soot Particles in a Laminar Premixed Flame: From Nucleation to Early Growth. *Combust. Flame* **2015**, *162*, 3854–3863.
- (87) Eberle, C.; Gerlinger, P.; Aigner, M. A Sectional PAH Model with Reversible PAH Chemistry for CFD Soot Simulations. *Combust. Flame* **2017**, *179*, 63–73.
- (88) Mao, Q.; van Duin, A. C. T.; Luo, K. H. Formation of Incipient Soot Particles from Polycyclic Aromatic Hydrocarbons: A ReaxFF Molecular Dynamics Study. *Carbon* **2017**, *121*, 380–388.
- (89) Johansson, K. O.; Dillstrom, T.; Elvati, P.; Campbell, M. F.; Schrader, P. E.; Popolan-Vaida, D. M.; Richards-Henderson, N. K.; Wilson, K. R.; Violi, A.; Michelsen, H. A. Radical-Radical Reactions, Pyrene Nucleation, and Incipient Soot Formation in Combustion. *Proc. Combust. Inst.* **2017**, *36*, 799–806.
- (90) Kholghy, M. R.; Eaves, N. A.; Veshkini, A.; Thomson, M. J. The Role of Reactive PAH Dimerization in Reducing Soot Nucleation Reversibility. *Proc. Combust. Inst.* **2019**, *37*, 1003–1011.
- (91) Mao, Q.; Zhou, J.; Luo, K. H.; van Duin, A. C. T. Atomistic Insights into the Dynamics of Binary Collisions between Gaseous Molecules and Polycyclic Aromatic Hydrocarbon Dimers. *Phys. Chem. Chem. Phys.* **2019**, *21*, 3849–3856.
- (92) Baron, P. A.; Willeke, K. Aerosol Fundamentals. In *Aerosol Measurement: Principles, Techniques, and Applications*, 2nd ed.; Baron, P. A.; Willeke, K., Eds.; Wiley and Sons: New York, 2001; pp 45–60.
- (93) Homann, K.-H.; Wagner, H. G. Some New Aspects of the Mechanism of Carbon Formation in Premixed Flames. *Symp. (Int.) Combust., [Proc.]* **1967**, *11*, 371–379.
- (94) Wersborg, B. L.; Howard, J. B.; Williams, G. C. Physical Mechanisms in Carbon Formation in Flames. *Symp. (Int.) Combust., [Proc.]* **1973**, *14*, 929–940.
- (95) Siegmann, K.; Sattler, K.; Siegmann, H. C. Clustering at High Temperatures: Carbon Formation in Combustion. *J. Electron Spectrosc. Relat. Phenom.* **2002**, *126*, 191–202.
- (96) Sabbah, H.; Biennier, L.; Klippenstein, S. J.; Sims, I. R.; Rowe, B. R. Exploring the Role of PAHs in the Formation of Soot: Pyrene Dimerization. *J. Phys. Chem. Lett.* **2010**, *1*, 2962–2967.
- (97) Camacho, J.; Lieb, S.; Wang, H. Evolution of Size Distribution of Nascent Soot in *n*- and *i*-Butanol Flames. *Proc. Combust. Inst.* **2013**, *34*, 1853–1860.
- (98) Eaves, N. A.; Dworkin, S. B.; Thomson, M. J. The Importance of Reversibility in Modeling Soot Nucleation and Condensation Processes. *Proc. Combust. Inst.* **2015**, *35*, 1787–1794.
- (99) Török, S.; Malmborg, V. B.; Simonsson, J.; Eriksson, A.; Martinsson, J.; Mannazhi, M.; Pagels, J.; Bengtsson, P.-E. Investigation of the Absorption Ångström Exponent and Its Relation to Physicochemical Properties for Mini-Cast Soot. *Aerosol Sci. Technol.* **2018**, *52*, 757–767.
- (100) Abraham, F. F. *Homogeneous Nucleation Theory: The Pretransition Theory of Vapor Condensation*; Academic Press: New York, 1974.
- (101) Pauling, L. *The Nature of the Chemical Bond*, 3rd ed.; Cornell University Press: Ithaca, NY, 1960.
- (102) Atkins, P. W. *Physical Chemistry*, 4th ed.; Freeman and Company: New York, 1990; p 604–605, 738–739.
- (103) McQuarrie, D. A.; Simon, J. D. *Physical Chemistry: A Molecular Approach*; University Science Books: Sausalito, CA, 1997.

- (104) Berry, R. S.; Rice, S. A.; Ross, J. *Physical Chemistry*, 2nd ed.; Oxford University Press: New York, 2000.
- (105) Levine, I. N. *Physical Chemistry*, 6th ed.; McGraw Hill: Boston, MA, 2009.
- (106) Heaven, M. C. Spectroscopy and Dynamics of Open-Shell Van Der Waals Molecules. *Annu. Rev. Phys. Chem.* **1992**, *43*, 283–310.
- (107) Dubernet, M.-L.; Flower, D.; Hutson, J. M. The Dynamics of Open-Shell Van Der Waals Complexes. *J. Chem. Phys.* **1991**, *94*, 7602–7618.
- (108) Dubernet, M.-L.; Hutson, J. M. Atom-Molecule Van Der Waals Complexes Containing Open-Shell Atoms. I. General Theory and Bending Levels. *J. Chem. Phys.* **1994**, *101*, 1939–1958.
- (109) Dubernet, M.-L.; Hutson, J. M. Atom-Molecule Van Der Waals Complexes Containing Open-Shell Atoms. 2. The Bound States of Cl-HCl. *J. Phys. Chem.* **1994**, *98*, 5844–5854.
- (110) Harris, S. J.; Kennedy, I. M. The Coagulation of Soot Particles with Van Der Waals Forces. *Combust. Sci. Technol.* **1988**, *59*, 443–454.
- (111) Vander Wal, R. L.; Yezzerets, A.; Currier, N. W.; Kim, D. H.; Wang, C. M. HRTEM Study of Diesel Soot Collected from Diesel Particulate Filters. *Carbon* **2007**, *45*, 70–77.
- (112) Vander Wal, R. L.; Tomasek, A. J. Soot Nanostructure: Dependence Upon Synthesis Conditions. *Combust. Flame* **2004**, *136*, 129–140.
- (113) Alfè, M.; Apicella, B.; Barbella, R.; Rouzaud, J.-N.; Tregrossi, A.; Ciajolo, A. Structure-Property Relationship in Nanostructures of Young and Mature Soot in Premixed Flames. *Proc. Combust. Inst.* **2009**, *32*, 697–704.
- (114) Lester, T. W.; Wittig, S. L. K. Soot Nucleation Kinetics in Premixed Methane Combustion. *Symp. (Int.) Combust., [Proc.]* **1977**, *16*, 671–680.
- (115) Rohlfing, E. A.; Chandler, D. W. Two-Color Pyrometric Imaging of Laser-Heated Carbon Particles in a Supersonic Flow. *Chem. Phys. Lett.* **1990**, *170*, 44–50.
- (116) McKinnon, J. T.; Howard, J. B. Application of Soot Formation Model: Effects of Chlorine. *Combust. Sci. Technol.* **1990**, *74*, 175–197.
- (117) Olofsson, N.-E.; Simonsson, J.; Török, S.; Bladh, H.; Bengtsson, P.-E. Evolution of Properties of Aging Soot in Premixed Flat Flames Studied by Laser-Induced Incandescence and Elastic Light Scattering. *Appl. Phys. B: Lasers Opt.* **2015**, *119*, 669–683.
- (118) Kholghy, M. R.; Afarin, Y.; Sediako, A. D.; Barba, J.; Lapuerta, M.; Chu, C.; Weingarten, J.; Borshanpour, B.; Chernov, V.; Thomson, M. J. Comparison of Multiple Diagnostic Techniques to Study Soot Formation and Morphology in a Diffusion Flame. *Combust. Flame* **2017**, *176*, 567–583.
- (119) Schenk, M.; Lieb, S.; Vieker, H.; Beyer, A.; Gölzhäuser, A.; Wang, H.; Kohse-Höinghaus, K. Imaging Nanocarbon Materials: Soot Particles in Flames Are Not Structurally Homogeneous. *ChemPhys Chem* **2013**, *14*, 3248–3254.
- (120) Yokelson, R. J.; Bertschi, I. T.; Christian, T. J.; Hobbs, P. V.; Ward, D. E.; Hao, W. M. Trace Gas Measurements in Nascent, Aged, and Cloud-Processed Smoke from African Savanna Fires by Airborne Fourier Transform Infrared Spectroscopy (AFTIR). *J. Geophys. Res.* **2003**, *108*, 8478.
- (121) Christian, T. J.; Kleiss, B.; Yokelson, R. J.; Holzinger, R.; Crutzen, P. J.; Hao, W. M.; Saharjo, B. H.; Ward, D. E. Comprehensive Laboratory Measurements of Biomass-Burning Emissions: 1. Emissions from Indonesian, African and Other Fuels. *J. Geophys. Res.* **2003**, *108*, 4719.
- (122) Akagi, S. K.; Craven, J. S.; Taylor, J. W.; McMeeking, G. R.; Yokelson, R. J.; Burling, I. R.; Urbanski, S. P.; Wold, C. E.; Seinfeld, J. H.; Coe, H.; Alvarado, M. J.; Weise, D. R. Evolution of Trace Gases and Particles Emitted by a Chaparral Fire in California. *Atmos. Chem. Phys.* **2012**, *12*, 1397–1421.
- (123) China, S.; Kulkarni, G.; Scarnato, B. V.; Sharma, N.; Pekour, M.; Shilling, J. E.; Wilson, J.; Zelenyuk, A.; Chand, D.; Liu, S.; Aiken, A. C.; Dubey, M.; Laskin, A.; Zaveri, R.; Mazzoleni, C. Morphology of Diesel Soot Residuals from Supercooled Water Droplets and Ice Crystals: Implications for Optical Properties. *Environ. Res. Lett.* **2015**, *10*, 114010.
- (124) Ahern, A. T.; Subramanian, R.; Saliba, G.; Lipsky, E. M.; Donahue, N. M.; Sullivan, R. C. Effect of Secondary Organic Aerosol Coating Thickness on the Real-Time Detection and Characterization of Biomass-Burning Soot by Two Particle Mass Spectrometers. *Atmos. Meas. Tech.* **2016**, *9*, 6117–6137.
- (125) Ahern, A. T.; Goldberger, L.; Jahl, L.; Thornton, J.; Sullivan, R. C. Production of  $\text{N}_2\text{O}_5$  and  $\text{ClNO}_2$  through Nocturnal Processing of Biomass-Burning Aerosol. *Environ. Sci. Technol.* **2018**, *52*, 550–559.
- (126) Sumlin, J. J.; Oxford, C. R.; Seo, B.; Pattison, R. R.; Williams, B. J.; Chakrabarty, R. K. Density and Homogeneous Internal Composition of Primary Brown Carbon Aerosol. *Environ. Sci. Technol.* **2018**, *52*, 3982.
- (127) Hou, L.-T.; Willis, R. A. Effect of Cigarette-Smoke Condensates on Homografts of Embryonic Lung Tissue in Rats. *J. Pathol. Bacteriol.* **1963**, *86*, 199–207.
- (128) Wooten, J. B. Gas-Phase Radicals in Cigarette Smoke: A Re-Evaluation of the Steady-State Model and the Cambridge Filter Pad. *Mini-Rev. Org. Chem.* **2011**, *8*, 412–426.
- (129) D'Alessio, A.; D'Anna, A.; D'Orsi, A.; Minutolo, P.; Barbella, R.; Ciajolo, A. Precursor Formation and Soot Inception in Premixed Ethylene Flames. *Symp. (Int.) Combust., [Proc.]* **1992**, *24*, 973–980.
- (130) Barone, A. C.; D'Alessio, A.; D'Anna, A. Morphological Characterization of the Early Process of Soot Formation by Atomic Force Microscopy. *Combust. Flame* **2003**, *132*, 181–187.
- (131) D'Anna, A.; Commodo, M.; Violi, S.; Allouis, C.; Kent, J. Nano Organic Carbon and Soot in Turbulent Non-Premixed Ethylene Flames. *Proc. Combust. Inst.* **2007**, *31*, 621–629.
- (132) Dobbins, R. A.; Megaridis, C. M. Morphology of Flame-Generated Soot as Determined by Thermophoretic Sampling. *Langmuir* **1987**, *3*, 254–259.
- (133) Commodo, M.; Violi, S.; D'Anna, A.; D'Alessio, A.; Allouis, C.; Beretta, F.; Minutolo, P. Soot and Nanoparticle Formation in Laminar and Turbulent Flames. *Combust. Sci. Technol.* **2007**, *179*, 387–400.
- (134) Stirn, R.; Baquet, T. G.; Kanjarkar, S.; Meier, W.; Geigle, K. P.; Grotheer, H. H.; Wahl, C.; Aigner, M. Comparison of Particle Size Measurements with Laser-Induced Incandescence, Mass Spectroscopy, and Scanning Mobility Particle Sizing in a Laminar Premixed Ethylene/Air Flame. *Combust. Sci. Technol.* **2009**, *181*, 329–349.
- (135) Grotheer, H. H.; Wolf, K.; Hoffmann, K. Photoionization Mass Spectrometry for the Investigation of Combustion Generated Nascent Nanoparticles and Their Relation to Laser Induced Incandescence. *Appl. Phys. B: Lasers Opt.* **2011**, *104*, 367–383.
- (136) Sirignano, M.; Bartos, D.; Conturso, M.; Dunn, M.; D'Anna, A.; Masri, A. R. Detection of Nanostructures and Soot in Laminar Premixed Flames. *Combust. Flame* **2017**, *176*, 299–308.
- (137) De Falco, G.; Sirignano, M.; Commodo, M.; Merotto, L.; Migliorini, F.; Dondé, R.; De Iuliis, S.; Minutolo, P.; D'Anna, A. Experimental and Numerical Study of Soot Formation and Evolution in Co-Flow Laminar Partially Premixed Flames. *Fuel* **2018**, *220*, 396–402.
- (138) Ishiguro, T.; Takatori, Y.; Akihama, K. Microstructure of Diesel Soot Particles Probed by Electron Microscopy: First Observation of Inner Core and Outer Shell. *Combust. Flame* **1997**, *108*, 231–234.
- (139) Hurt, R. H.; Crawford, G. P.; Shim, H.-S. Equilibrium Nanostructure of Primary Soot Particles. *Proc. Combust. Inst.* **2000**, *28*, 2539–2546.
- (140) Chen, H. X.; Dobbins, R. A. Crystallogenesis of Particles Formed in Hydrocarbon Combustion. *Combust. Sci. Technol.* **2000**, *159*, 109–128.
- (141) Shaddix, C. R.; Palotás, Á. B.; Megaridis, C. M.; Choi, M. Y.; Yang, N. Y. C. Soot Graphitic Order in Laminar Diffusion Flames and a Large-Scale JP-8 Pool Fire. *Int. J. Heat Mass Transfer* **2005**, *48*, 3604–3614.

- (142) Vander Wal, R. L.; Bryg, V. M.; Huang, C.-H. Insights into the Combustion Chemistry within a Gas-Turbine Driven Auxiliary Power Unit as a Function of Fuel Type and Power Level Using Soot Nanostructure as a Tracer. *Fuel* **2014**, *115*, 282–287.
- (143) Seong, H.; Choi, S.; Lee, K. Examination of Nanoparticles from Gasoline Direct-Injection (GDI) Engines Using Transmission Electron Microscopy (TEM). *Int. J. Auto. Technol.* **2014**, *15*, 175–181.
- (144) Toth, P.; Palotas, A. B.; Ring, T. A.; Eddings, E. G.; Vander Wal, R. L.; Lighty, J. S. The Effect of Oxidation Pressure on the Equilibrium Nanostructure of Soot Particles. *Combust. Flame* **2015**, *162*, 2422–2430.
- (145) La Rocca, A.; Bonatesta, F.; Fay, M.W.; Campanella, F. Characterisation of Soot in Oil from a Gasoline Direct Injection Engine Using Transmission Electron Microscopy. *Tribol. Int.* **2015**, *86*, 77–84.
- (146) Ulrich, G. D.; Subramanian, N. S. Particle Growth in Flames. III. Coalescence as a Rate-Controlling Process. *Combust. Sci. Technol.* **1977**, *17*, 119–126.
- (147) Forrest, S. R.; Witten, T. A., Jr. Long-Range Correlations in Smoke-Particle Aggregates. *J. Phys. A: Math. Gen.* **1979**, *12*, L109–L117.
- (148) Wagner, H. Gg. Soot Formation in Combustion. *Symp. (Int.) Combust., [Proc.]* **1979**, *17*, 3–19.
- (149) Miodownik, M. *Liquid Rules: The Delightful and Dangerous Substances That Flow through Our Lives*; Houghton Mifflin Harcourt: Boston, 2019.
- (150) Maricq, M. M. Coagulation Dynamics of Fractal-Like Soot Aggregates. *J. Aerosol Sci.* **2007**, *38*, 141–156.
- (151) Graham, S. C. The Collisional Growth of Soot Particles at High Temperatures. *Symp. (Int.) Combust., [Proc.]* **1977**, *16*, 663–669.
- (152) Prado, G. P.; Lee, M. L.; Hites, R. A.; Hoult, D. P.; Howard, J. B. Soot and Hydrocarbon Formation in a Turbulent Diffusion Flame. *Symp. (Int.) Combust., [Proc.]* **1977**, *16*, 649–661.
- (153) Saffaripour, M.; Veshkini, A.; Kholghy, M. R.; Thomson, M. J. Experimental Investigation and Detailed Modeling of Soot Aggregate Formation and Size Distribution in Laminar Coflow Diffusion Flames of Jet A-1, a Synthetic Kerosene, and *n*-Decane. *Combust. Flame* **2014**, *161*, 848–863.
- (154) Veshkini, A.; Dworkin, S. B.; Thomson, M. J. Understanding Soot Particle Size Evolution in Laminar Ethylene/Air Diffusion Flames Using Novel Soot Coalescence Models. *Combust. Theory Model.* **2016**, *20*, 707–734.
- (155) Hou, D.; Chu, Q.; Chen, D.; Pascazio, L.; Kraft, M.; You, X., Atomic Insights into the Sintering Process of Polycyclic Aromatic Hydrocarbon Clusters. *Proc. Combust. Inst.* **2020**, *38*, in press. DOI: 10.1016/j.proci.2020.06.368.
- (156) Wagner, H. Gg. Soot Formation: An Overview. In *Particulate Carbon, Formation During Combustion*; Siegla, D. C.; Smith, G. W., Eds.; Springer: New York, 1981; pp 1–30.
- (157) Aubagnac-Karkar, D.; El Bakali, A.; Desgroux, P. Soot Particles Inception and PAH Condensation Modelling Applied in a Soot Model Utilizing a Section Method. *Combust. Flame* **2018**, *189*, 190–206.
- (158) Bisetti, F.; Blanquart, G.; Mueller, M. E.; Pitsch, H. On the Formation and Early Evolution of Soot in Turbulent Nonpremixed Flames. *Combust. Flame* **2012**, *159*, 317–335.
- (159) Çengel, Y. A.; Boles, M. A. *Thermodynamics: An Engineering Approach*, 8th ed.; McGraw-Hill Education: New York, 2015; p 996.
- (160) Kaye, G. W. C.; Ewen, D. The Sublimation of Metals at Low Pressures. *Proc. R. Soc. A* **1913**, *89*, 58–67.
- (161) Zangwill, A. *Physics at Surfaces*; University Press: Cambridge, 1988.
- (162) Vidali, G.; Ihm, G.; Kim, H.-Y.; Cole, M. W. Potentials of Physical Adsorption. *Surf. Sci. Rep.* **1991**, *12*, 135–181.
- (163) Winn, J. S. *Physical Chemistry*; HarperCollins: New York, 1995.
- (164) Zacharia, R.; Ulbricht, H.; Hertel, T. Interlayer Cohesive Energy of Graphite from Thermal Desorption of Polyaromatic Hydrocarbons. *Phys. Rev. B: Condens. Matter Mater. Phys.* **2004**, *69*, 155406.
- (165) Bedjanian, Y.; Nguyen, M. L.; Guilloteau, A. Desorption of Polycyclic Aromatic Hydrocarbons from Soot Surface: Five- and Six-Ring ( $C_{22}$ ,  $C_{24}$ ) PAHs. *J. Phys. Chem. A* **2010**, *114*, 3533–3539.
- (166) Björk, J.; Hanke, F.; Palma, C.-A.; Samori, P.; Cecchini, M.; Persson, M. Adsorption of Aromatic and Anti-Aromatic Systems on Graphene through  $\Pi$ - $\Pi$  Stacking. *J. Phys. Chem. Lett.* **2010**, *1*, 3407–3412.
- (167) Tournus, F.; Latil, S.; Heggie, M. I.; Charlier, J.-C.  $\Pi$ -Stacking Interactions between Carbon Nanotubes and Organic Molecules. *Phys. Rev. B: Condens. Matter Mater. Phys.* **2005**, *72*, 075431.
- (168) Barker, J. A.; Everett, D. H. High Temperature Adsorption and the Determination of the Surface Area of Solids. *Trans. Faraday Soc.* **1962**, *58*, 1608–1623.
- (169) Nørskov, J. K. Chemisorption at Metal Surfaces. *Rep. Prog. Phys.* **1990**, *53*, 1253–1295.
- (170) Ledovskikh, A.; Danilov, D.; Notten, P. H. L. Equilibrium Kinetics of Chemisorption Processes. *ChemPhysChem* **2008**, *9*, 1040–1045.
- (171) Aakko-Saksa, P. T.; Cook, C.; Kiviaho, J.; Repo, T. Liquid Organic Hydrogen Carriers for Transportation and Storing of Renewable Energy - Review and Discussion. *J. Power Sources* **2018**, *396*, 803–823.
- (172) Ruffieux, P.; Gröning, O.; Bielmann, M.; Gröning, P. Hydrogen Chemisorption on  $sp^2$ -Bonded Carbon: Influence of the Local Curvature and Local Electronic Effects. *Appl. Phys. A: Mater. Sci. Process.* **2004**, *78*, 975–980.
- (173) Sendt, K.; Haynes, B. S. Density Functional Study of the Chemisorption of  $O_2$  across Two Rings of the Armchair Surface of Graphite. *J. Phys. Chem. C* **2007**, *111*, 5465–5473.
- (174) Smith, J. R. *Theory of Chemisorption*; Springer-Verlag: Berlin, 1980.
- (175) Netzer, L.; Iscovici, R.; Sagiv, J. Adsorbed Monolayers Versus Langmuir-Blodgett Monolayers - Why and How? I: From Monolayer to Multilayer, by Adsorption. *Thin Solid Films* **1983**, *99*, 235–241.
- (176) Singh, U. K.; Vannice, M. A. Kinetics of Liquid-Phase Hydrogenation Reactions over Supported Metal Catalysts: A Review. *Appl. Catal., A* **2001**, *213*, 1–24.
- (177) Michelsen, H. A.; Rettner, C. T.; Auerbach, D. J. The Adsorption of Hydrogen at Copper Surfaces: A Model System for the Study of Activated Adsorption. In *Surface Reactions*; Madix, R. J., Ed.; Springer-Verlag: New York, 1994.
- (178) Newns, D. M. Self-Consistent Model of Hydrogen Chemisorption. *Phys. Rev.* **1969**, *178*, 1123–1135.
- (179) Chakrapani, N.; Zhang, Y. M.; Nayak, S. K.; Moore, J. A.; Carroll, D. L.; Choi, Y. Y.; Ajayan, P. M. Chemisorption of Acetone on Carbon Nanotubes. *J. Phys. Chem. B* **2003**, *107*, 9308–9311.
- (180) Mikhailov, E. F.; Vlasenko, S. S.; Krämer, L.; Niessner, R. Interaction of Soot Aerosol Particles with Water Droplets: Influence of Surface Hydrophilicity. *J. Aerosol Sci.* **2001**, *32*, 697–711.
- (181) Franklin, R. E. Crystallite Growth in Graphitizing and Non-Graphitizing Carbon. *Proc. R. Soc. London, Series A* **1951**, *209*, 196–218.
- (182) Franklin, R. E. Homogeneous and Heterogeneous Graphitization of Carbon. *Nature* **1956**, *177*, 239.
- (183) Oberlin, A. Carbonization and Graphitization. *Carbon* **1984**, *22*, 521–541.
- (184) Emmerich, F. G. Evolution of Heat Treatment of Crystallinity in Carbons. *Carbon* **1995**, *33*, 1709–1715.
- (185) Palotás, Á. B.; Rainey, L. C.; Sarofim, A. F.; Vander Sande, J. B.; Ciambelli, P. Effect of Oxidation on the Microstructure of Carbon Blacks. *Energy Fuels* **1996**, *10*, 254–259.
- (186) Russo, C.; Alfé, M.; Rouzaud, J.-N.; Stanzione, F.; Tregrossi, A.; Ciajolo, A. Probing Structures of Soot Formed in Premixed Flames of Methane, Ethylene, and Benzene. *Proc. Combust. Inst.* **2013**, *34*, 1885–1892.

- (187) Apicella, B.; Ciajolo, A.; Tregrossi, A.; Abrahamson, J.; Vander Wal, R. L.; Russo, C. HRTEM and EELS Investigation of Flame-Formed Soot Nanostructure. *Fuel* **2018**, *225*, 218–224.
- (188) Thrower, P. A.; Mayer, R. M. Point Defects and Self-Diffusion in Graphite. *Phys. Status Solidi A* **1978**, *47*, 11–37.
- (189) Franklin, R. E. The Interpretation of Diffuse X-Ray Diagrams of Carbon. *Acta Crystallogr.* **1950**, *3*, 107–121.
- (190) Franklin, R. E. The Structure of Graphitic Carbons. *Acta Crystallogr.* **1951**, *4*, 253–261.
- (191) Dobbins, R. A.; Govatzidakis, G. J.; Lu, W.; Schwartzman, A. F.; Fletcher, R. A. Carbonization Rate of Soot Precursor Particles. *Combust. Sci. Technol.* **1996**, *121*, 103–121.
- (192) Vander Wal, R. L. A TEM Methodology for the Study of Soot Particle Structure. *Combust. Sci. Technol.* **1997**, *126*, 333–357.
- (193) Agullo-Lopez, F.; Catlow, C. R. A.; Townsend, P. D. *Point Defects in Materials*; Academic Press: San Diego, CA, 1988.
- (194) Gersten, J. I.; Smith, F. W. *The Physics and Chemistry of Materials*; John Wiley & Sons, Inc.: New York, 2001.
- (195) Lehmann, C. *Interactions of Radiation with Solids and Elementary Defect Production*; Elsevier North-Holland Inc.: New York, 1977; p 341.
- (196) Balluffi, R. W.; Granato, A. V. Dislocations, Vacancies, and Interstitials. In *Dislocations in Solids*; Nabarro, F. R. N., Ed.; Elsevier North-Holland, Inc.: New York, 1979; Vol. 4.
- (197) Michelsen, H. A. Understanding and Predicting the Temporal Response of Laser-Induced Incandescence from Carbonaceous Particles. *J. Chem. Phys.* **2003**, *118*, 7012–7045.
- (198) Banhart, F.; Füller, T.; Redlich, P.; Ajayan, P. M. The Formation, Annealing and Self-Compression of Carbon Onions under Electron Irradiation. *Chem. Phys. Lett.* **1997**, *269*, 349–355.
- (199) Sigle, W.; Redlich, P. Point Defect Concentration Development in Electron-Irradiated Bucky Onions. *Philos. Mag. Lett.* **1997**, *76*, 125–132.
- (200) Wersborg, B. L.; Fox, L. K.; Howard, J. B. Soot Concentration and Absorption Coefficient in a Low-Pressure Flame. *Combust. Flame* **1975**, *24*, 1–10.
- (201) Apicella, B.; Pré, P.; Alfe, M.; Ciajolo, A.; Gargiulo, V.; Russo, C.; Tregrossi, A.; Deldique, D.; Rouzaud, J.-N. Soot Nanostructure Evolution in Premixed Flames by High Resolution Electron Transmission Microscopy (HRTEM). *Proc. Combust. Inst.* **2015**, *35*, 1895–1902.
- (202) Li, J.; Yu, S. Soot Particles Analysis in Laminar Premixed Propane/Oxygen ( $C_3H_8/O_2$ ) Flame Using Published Measurement Data. *China Particulol.* **2003**, *1*, 168–171.
- (203) Wu, J.-S.; Krishnan, S. S.; Faeth, G. M. Refractive Indices at Visible Wavelengths of Soot Emitted from Buoyant Turbulent Diffusion Flames. *J. Heat Transfer* **1997**, *119*, 230–237.
- (204) Michelsen, H. A. Effects of Maturity and Temperature on Soot Density and Specific Heat. *Proc. Combust. Inst.* **2020**, *38*, in press. DOI: [10.1016/j.proci.2020.06.383](https://doi.org/10.1016/j.proci.2020.06.383).
- (205) Santamaría, A.; Mondragón, F.; Quiñónez, W.; Eddings, E. G.; Sarofim, A. F. Average Structural Analysis of the Extractable Material of Young Soot Gathered in an Ethylene Inverse Diffusion Flame. *Fuel* **2007**, *86*, 1908–1917.
- (206) Velásquez, M.; Mondragón, F.; Santamaría, A. Chemical Characterization of Soot Precursors and Soot Particles Produced in Hexane and Diesel Surrogates Using an Inverse Diffusion Flame Burner. *Fuel* **2013**, *104*, 681–690.
- (207) Apicella, B.; Alfe, M.; Barbella, R.; Tregrossi, A.; Ciajolo, A. Aromatic Structures of Carbonaceous Materials and Soot Inferred by Spectroscopic Analysis. *Carbon* **2004**, *42*, 1583–1589.
- (208) Migliorini, F.; Thomson, K. A.; Smallwood, G. J. Investigation of the Optical Properties of Aging Soot. *Appl. Phys. B: Lasers Opt.* **2011**, *104*, 273–283.
- (209) Lahaye, J. Mechanisms of Soot Formation. *Polym. Degrad. Stab.* **1990**, *30*, 111–121.
- (210) Appel, J.; Bockhorn, H.; Frenklach, M. Kinetic Modeling of Soot Formation with Detailed Chemistry and Physics: Laminar Premixed Flames of C<sub>2</sub> Hydrocarbons. *Combust. Flame* **2000**, *121*, 122–136.
- (211) Khosousi, A.; Dworkin, S. B. Soot Surface Reactivity During Surface Growth and Oxidation in Laminar Diffusion Flames. *Combust. Flame* **2015**, *162*, 4523–4532.
- (212) Singh, J.; Balthasar, M.; Kraft, M.; Wagner, W. Stochastic Modeling of Soot Particle Size and Age Distributions in Laminar Premixed Flames. *Proc. Combust. Inst.* **2005**, *30*, 1457–1465.
- (213) Smooke, M. D.; Long, M. B.; Connelly, B. C.; Colket, M. B.; Hall, R. J. Soot Formation in Laminar Diffusion Flames. *Combust. Flame* **2005**, *143*, 613–628.
- (214) Blanquart, G.; Pitsch, H. Analyzing the Effects of Temperature on Soot Formation with a Joint Volume-Surface-Hydrogen Model. *Combust. Flame* **2009**, *156*, 1614–1626.
- (215) Blanquart, G.; Pitsch, H. A Joint Vol.-Surface-Hydrogen Multi-Variate Model for Soot Formation. In *Combustion Generated Fine Carbonaceous Particles*; Bockhorn, H.; D'Anna, A.; Sarofim, A. F.; Wang, H., Eds.; KIT Scientific Publishing: Karlsruhe, Germany, 2009; pp 437–463. <https://publikationen.bibliothek.kit.edu/1000013744> (accessed 2020-09-30)
- (216) Finlayson-Pitts, B. J.; Pitts, J. N., Jr. *Chemistry of the Upper and Lower Atmosphere*; Academic Press, San Diego, CA, 2000.
- (217) Seinfeld, J. H.; Pandis, S. N. *Atmospheric Chemistry and Physics from Air Pollution to Climate Change*; John Wiley and Sons: New York, 1998; pp 596–607.
- (218) Chen, D.; Zainuddin, Z.; Yapp, E.; Akroyd, J.; Mosbach, S.; Kraft, M. A Fully Coupled Simulation of PAH and Soot Growth with a Population Balance Model. *Proc. Combust. Inst.* **2013**, *34*, 1827–1835.
- (219) Wang, M.; Tang, Q.; Mei, J.; You, X. On the Effective Density of Soot Particles in Premixed Ethylene Flames. *Combust. Flame* **2018**, *198*, 428–435.
- (220) Mitchell, P.; Frenklach, M. Particle Aggregation with Simultaneous Surface Growth. *Phys. Rev. E: Stat. Phys., Plasmas, Fluids, Relat. Interdiscip. Top.* **2003**, *67*, 061407.
- (221) Fang, Z. Z. *Sintering of Advanced Materials: Fundamentals and Processes*; Woodhead Publishing Limited: Oxford, 2010.
- (222) Merriam-Webster Dictionary; Merriam-Webster, Inc.: Springfield, MA, 2019.
- (223) Charalampopoulos, T. T.; Felske, J. D. Refractive Indices of Soot Particles Deduced from *In-Situ* Laser Light Scattering Measurements. *Combust. Flame* **1987**, *68*, 283–294.
- (224) Williams, T. C.; Shaddix, C. R.; Jensen, K. A.; Suo-Anttila, J. M. Measurement of the Dimensionless Extinction Coefficient of Soot within Laminar Diffusion Flames. *Int. J. Heat Mass Transfer* **2007**, *50*, 1616–1630.
- (225) López-Yglesias, X.; Schrader, P. E.; Michelsen, H. A. Soot Maturity and Absorption Cross Sections. *J. Aerosol Sci.* **2014**, *75*, 43–64.
- (226) Michelsen, H. A.; Schulz, C.; Smallwood, G. J.; Will, S. Laser-Induced Incandescence: Particle Diagnostics for Combustion, Atmospheric, and Industrial Applications. *Prog. Energy Combust. Sci.* **2015**, *51*, 2–48.
- (227) Jung, Y.; Bae, C. Immaturity of Soot Particles in Exhaust Gas for Low Temperature Diesel Combustion in a Direct Injection Compression Ignition Engine. *Fuel* **2015**, *161*, 312–322.
- (228) Leschowski, M.; Thomson, K. A.; Snelling, D. R.; Schulz, C.; Smallwood, G. J. Combination of LII and Extinction Measurements for Determination of Soot Volume Fraction and Estimation of Soot Maturity in Non-Premixed Laminar Flames. *Appl. Phys. B: Lasers Opt.* **2015**, *119*, 685–696.
- (229) Yon, J.; Therssen, E.; Liu, F.; Bejaoui, S.; Hebert, D. Influence of Soot Aggregate Size and Internal Multiple Scattering on LII Signal and the Absorption Function Variation with Wavelength Determined by the TEW-LII Method. *Appl. Phys. B: Lasers Opt.* **2015**, *119*, 643–655.
- (230) Alexandrino, K.; Salinas, J.; Miller, Á.; Bilbao, R.; Alzueta, M. U. Sooting Propensity of Dimethyl Carbonate, Soot Reactivity and Characterization. *Fuel* **2016**, *183*, 64–72.

- (231) Cenker, E.; Roberts, W. L. Quantitative Effects of Rapid Heating on Soot-Particle Sizing through Analysis of Two-Pulse LII. *Appl. Phys. B: Lasers Opt.* **2017**, *123*, 74.
- (232) Sediako, A. D.; Soong, C.; Howe, J. Y.; Kholghy, M. R.; Thomson, M. J. Real-Time Observation of Soot Aggregate Oxidation in an Environmental Transmission Electron Microscope. *Proc. Combust. Inst.* **2017**, *36*, 841–851.
- (233) Andreae, M. O.; Gelencsér, A. Black Carbon or Brown Carbon? The Nature of Light-Absorbing Carbonaceous Aerosols. *Atmos. Chem. Phys.* **2006**, *6*, 3131–3148.
- (234) Maricq, M. M. Chemical Characterization of Particulate Emissions from Diesel Engines: A Review. *J. Aerosol Sci.* **2007**, *38*, 1079–1118.
- (235) Le, K. C.; Pino, T.; Pham, V. T.; Henriksson, T.; Török, S.; Bengtsson, P.-E. Raman Spectroscopy of Mini-Cast Soot with Various Fractions of Organic Compounds: Structural Characterization During Heating Treatment from 25 to 1000 °C. *Combust. Flame* **2019**, *209*, 291–302.
- (236) Laskin, A.; Laskin, J.; Nizkorodov, S. A. Chemistry of Atmospheric Brown Carbon. *Chem. Rev.* **2015**, *115*, 4335–4382.
- (237) Jiang, H.; Li, T.; Wang, Y.; He, P.; Wang, B. The Evolution of Soot Morphology and Nanostructure Along the Axial Direction in Diesel Spray Jet Flames. *Combust. Flame* **2019**, *199*, 204–212.
- (238) Bambha, R. P.; Michelsen, H. A. Effects of Aggregate Morphology and Size on Laser-Induced Incandescence and Scattering from Black Carbon (Mature Soot). *J. Aerosol Sci.* **2015**, *88*, 159–181.
- (239) Palmer, H. B.; Cullis, C. F. The Formation of Carbon from Gases. In *Chemistry and Physics of Carbon*; Marcel Dekker, Inc.: New York, 1965; Vol. 1, pp 265–325.
- (240) Park, S.-H.; Choi, M. Y.; Yozgatligil, A. Nanostructure of Soot Collected from Ethanol Droplet Flames in Microgravity. *Combust. Sci. Technol.* **2009**, *181*, 1164–1186.
- (241) Muñoz, R. H.; Charalampopoulos, T. T. Evolution of Compositional and Structural Properties of Soot in Premixed Alkane Flames. *Symp. (Int.) Combust., [Proc.]* **1998**, *27*, 1471–1479.
- (242) Lahaye, J.; Prado, G. Morphology and Internal Structure of Soot and Carbon Blacks. In *Particulate Carbon: Formation During Combustion*; Siegla, D. C., Smith, G. W., Eds.; Plenum: New York, 1981; pp 33–35.
- (243) Köylü, Ü. Ö.; Faeth, G. M. Structure and Overfire Soot in Buoyant Turbulent Diffusion Flames at Long Residence Times. *Combust. Flame* **1992**, *89*, 140–156.
- (244) Faeth, G. M.; Köylü, Ü. Ö. Soot Morphology and Optical Properties in Nonpremixed Turbulent Flame Environments. *Combust. Sci. Technol.* **1995**, *108*, 207–229.
- (245) Colbeck, I.; Atkinson, B.; Johar, Y. The Morphology and Optical Properties of Soot Produced by Different Fuels. *J. Aerosol Sci.* **1997**, *28*, 715–723.
- (246) Mouton, T.; Mercier, X.; Wartel, M.; Lamoureux, N.; Desgroux, P. Laser-Induced Incandescence Technique to Identify Soot Nucleation and Very Small Particles in Low-Pressure Methane Flames. *Appl. Phys. B: Lasers Opt.* **2013**, *112*, 369–379.
- (247) Bladh, H.; Olofsson, N.-E.; Mouton, T.; Simonsson, J.; Mercier, X.; Faccinetto, A.; Bengtsson, P.-E.; Desgroux, P. Probing the Smallest Soot Particles in Low-Sooting Premixed Flames Using Laser-Induced Incandescence. *Proc. Combust. Inst.* **2015**, *35*, 1843–1850.
- (248) Betrancourt, C.; Liu, F.; Desgroux, P.; Mercier, X.; Faccinetto, A.; Salamanca, M.; Ruwe, L.; Kohse-Höinghaus, K.; Emmrich, D.; Beyer, A.; Gölzhäuser, A.; Tritscher, T. Investigation of the Size of the Incandescent Incipient Soot Particles in Premixed Sooting and Nucleation Flames of *n*-butane Using LII, HIM, and 1 nm-SMPs. *Aerosol Sci. Technol.* **2017**, *51*, 916–935.
- (249) Desgroux, P.; Faccinetto, A.; Mercier, X.; Mouton, T.; Aubagnac Karkar, D.; El Bakali, A. Comparative Study of the Soot Formation Process in a “Nucleation” and a “Sooting” Low Pressure Premixed Methane Flame. *Combust. Flame* **2017**, *184*, 153–166.
- (250) Betrancourt, C.; Mercier, X.; Liu, F.; Desgroux, P. Quantitative Measurement of Volume Fraction Profiles of Soot of Different Maturities in Premixed Flames by Extinction-Calibrated Laser-Induced Incandescence. *Appl. Phys. B: Lasers Opt.* **2019**, *125*, DOI: 10.1007/s00340-018-7127-2.
- (251) Moallemi, A.; Kazemimanesh, M.; Kostiuk, L. W.; Olfert, J. S. The Effect of Sodium Chloride on the Nanoparticles Observed in a Laminar Methane Diffusion Flame. *Combust. Flame* **2018**, *188*, 273–283.
- (252) Buseck, P. R.; Adachi, K.; Gelencsér, A.; Tompa, É.; Pósfai, M. Ns-Soot: A Material-Based Term for Strong Light-Absorbing Carbonaceous Particles. *Aerosol Sci. Technol.* **2014**, *48*, 777–788.
- (253) Happonen, M.; Lähde, T.; Messing, M. E.; Sarjovaara, T.; Larmi, M.; Wallenberg, L. R.; Virtanen, A.; Keskinen, J. The Comparison of Particle Oxidation and Surface Structure of Diesel Soot Particles between Fossil Fuel and Novel Renewable Diesel Fuel. *Fuel* **2010**, *89*, 4008–4013.
- (254) Gaddam, C. K.; Vander Wal, R. L. Physical and Chemical Characterization of SIDI Engine Particulates. *Combust. Flame* **2013**, *160*, 2517–2528.
- (255) Jaramillo, I. C.; Gaddam, C. K.; Vander Wal, R. L.; Lighty, J. S. Effect of Nanostructure, Oxidative Pressure and Extent of Oxidation on Model Carbon Reactivity. *Combust. Flame* **2015**, *162*, 1848–1856.
- (256) Kim, H.; Kim, J. Y.; Kim, J. S.; Jin, H. C. Physicochemical and Optical Properties of Combustion-Generated Particles from Coal-Fired Power Plant, Automobiles, Ship Engines, and Charcoal Kilns. *Fuel* **2015**, *161*, 120–128.
- (257) Sirignano, M.; Kent, J.; D'Anna, A. Modeling Formation and Oxidation of Soot in Nonpremixed Flames. *Energy Fuels* **2013**, *27*, 2303–2315.
- (258) Millikan, R. C. Optical Properties of Soot. *J. Opt. Soc. Am.* **1961**, *51*, 698–699.
- (259) Minutolo, P.; Gambi, G.; D'Alessio, A. The Optical Band Gap Model in the Interpretation of the UV-Visible Absorption Spectra of Rich Premixed Flames. *Symp. (Int.) Combust., [Proc.]* **1996**, *26*, 951–957.
- (260) Siddall, R. G.; McGrath, I. A. The Emissivity of Luminous Flames. *Symp. (Int.) Combust., [Proc.]* **1963**, *9*, 102–110.
- (261) Dalzell, W. H.; Sarofim, A. F. Optical Constants of Soot and Their Application to Heat-Flux Calculations. *J. Heat Transfer* **1969**, *91*, 100–104.
- (262) D'Alessio, A.; Beretta, F.; Venitozzi, C. Optical Investigations of Soot Forming Methane-Oxygen Flames. *Combust. Sci. Technol.* **1972**, *5*, 263–272.
- (263) Habib, Z. G.; Vervisch, P. On the Refractive Index of Soot at Flame Temperature. *Combust. Sci. Technol.* **1988**, *59*, 261–274.
- (264) Manin, J.; Pickett, L. M.; Skeen, S. A. Two-Color Diffuse Back-Illuminated Imaging as a Diagnostic for Time-Resolved Soot Measurements in Reacting Sprays. *SAE Int. J. Engines* **2013**, *6*, 1908–1921.
- (265) Ma, B.; Long, M. B. Combined Soot Optical Characterization Using 2-D Multi-Angle Light Scattering and Spectrally Resolved Line-of-Sight Attenuation and Its Implications on Soot Color-Ratio Pyrometry. *Appl. Phys. B: Lasers Opt.* **2014**, *117*, 287–303.
- (266) Simonsson, J.; Olofsson, N.-E.; Török, S.; Bengtsson, P.-E.; Bladh, H. Wavelength Dependence of Extinction in Sooting Flat Premixed Flames in the Visible and near-Infrared Regimes. *Appl. Phys. B: Lasers Opt.* **2015**, *119*, 657–667.
- (267) Chang, H.; Charalampopoulos, T. T. Determination of the Wavelength Dependence of Refractive Indices of Flame Soot. *Proc. R. Soc. London, Series A* **1990**, *430*, 577–591.
- (268) Bohren, C. F.; Huffman, D. R. *Absorption and Scattering of Light by Small Particles*; John Wiley and Sons: New York, 1983.
- (269) da Rosa, A. *Fundamentals of Renewable Energy Processes*, 3rd ed.; Academic Press: Cambridge, MA, 2013; p 908.
- (270) Selamet, A.; Arpacı, V. S. Monochromatic Absorption of Luminous Flames. *Combust. Sci. Technol.* **1991**, *78*, 165–175.
- (271) Köylü, Ü. Ö. Quantitative Analysis of *In Situ* Optical Diagnostics for Inferring Particle/Aggregate Parameters in Flames: Implications for Soot Surface Growth and Total Emissivity. *Combust. Flame* **1997**, *109*, 488–500.

- (272) Köylü, Ü. Ö.; Faeth, G. M. Spectral Extinction Coefficients of Soot Aggregates from Turbulent Diffusion Flames. *J. Heat Transfer* **1996**, *118*, 415–421.
- (273) Bartos, D.; Sirignano, M.; Dunn, M. J.; D'Anna, A.; Masri, A. R. Soot Inception in Laminar Coflow Diffusion Flames. *Combust. Flame* **2019**, *205*, 180–192.
- (274) Goulay, F.; Schrader, P. E.; Michelsen, H. A. Effect of the Wavelength Dependence of the Emissivity on Inferred Soot Temperatures Measured by Spectrally Resolved Laser-Induced Incandescence. *Appl. Phys. B: Lasers Opt.* **2010**, *100*, 655–663.
- (275) Vander Wal, R. L. Laser-Induced Incandescence: Excitation and Detection Conditions, Material Transformations, and Calibration. *Appl. Phys. B: Lasers Opt.* **2009**, *96*, 601–611.
- (276) Liu, H.; Zhang, P.; Liu, X.; Chen, B.; Geng, C.; Li, B.; Wang, H.; Li, Z.; Yao, M. Laser Diagnostics and Chemical Kinetic Analysis of PAHs and Soot in Co-Flow Partially Premixed Flames Using Diesel Surrogate and Oxygenated Additives of *n*-Butanol and DMF. *Combust. Flame* **2018**, *188*, 129–141.
- (277) Goulay, F.; Nemes, L.; Schrader, P. E.; Michelsen, H. A. Spontaneous Emission from  $C_2(D\ ^3\Pi_G)$  and  $C_3(a\ ^1\Pi_U)$  During Laser Irradiation of Soot Particles. *Mol. Phys.* **2010**, *108*, 1013–1025.
- (278) Karatas, A. E.; Gülder, Ö. L. Soot Formation in High Pressure Laminar Diffusion Flames. *Prog. Energy Combust. Sci.* **2012**, *38*, 818–845.
- (279) Robertson, J. Amorphous Carbon. *Adv. Phys.* **1986**, *35*, 317–374.
- (280) Dresselhaus, M. S.; Dresselhaus, G.; Eklund, P. C. *Science of Fullerenes and Carbon Nanotubes*; Academic Press: San Diego, 1996; p 965.
- (281) McNaught, A. D.; Wilkinson, A. *IUPAC Compendium of Chemical Terminology*, 2nd ed. (the “Gold Book”); IUPAC: Research Triangle Park, NC. DOI: [10.1351/goldbook](https://doi.org/10.1351/goldbook) (accessed 2020-09-30).
- (282) Allen, M. J.; Tung, V. C.; Kaner, R. B. Honeycomb Carbon: A Review of Graphene. *Chem. Rev.* **2010**, *110*, 132–145.
- (283) Chung, D. D. L. Review Graphite. *J. Mater. Sci.* **2002**, *37*, 1475–1489.
- (284) Yamada, S.; Sato, H. Some Physical Properties of Glassy Carbon. *Nature* **1962**, *193*, 261–262.
- (285) Coward, F. C.; Lewis, J. C. Vitreous Carbon: A New Form of Carbon. *J. Mater. Sci.* **1967**, *2*, 507–512.
- (286) Harris, P. J. F. Fullerene-Related Structure of Commercial Glassy Carbons. *Philos. Mag.* **2004**, *84*, 3159–3167.
- (287) Bauer, J.; Schroer, A.; Schwaiger, R.; Kraft, O. Approaching Theoretical Strength in Glassy Carbon Nanolattices. *Nat. Mater.* **2016**, *15*, 438–443.
- (288) Greiner, N. R.; Phillips, D. S.; Johnson, J. D.; Volk, F. Diamonds in Detonation Soot. *Nature* **1988**, *333*, 440–442.
- (289) Kuznetsov, V. L.; Chuvilin, A. L.; Moroz, E. M.; Kolomiichuk, V. N.; Shaikhutdinov, S. K.; Butenko, Y. V.; Mal'kov, I. Y. Effect of Explosion Conditions on the Structure of Detonation Soots: Ultradisperse Diamond and Onion Carbon. *Carbon* **1994**, *32*, 873–882.
- (290) Chen, P.; Huang, F.; Yun, S. Characterization of the Condensed Carbon in Detonation Soot. *Carbon* **2003**, *41*, 2093–2099.
- (291) Watkins, E. B.; Velizhanin, K. A.; Dattelbaum, D. M.; Gustavsen, R. L.; Aslam, T. D.; Podlesak, D. W.; Huber, R. C.; Firestone, M. A.; Ringstrand, B. S.; Willey, T. M.; Bagge-Hansen, M.; Hodgin, R.; Lauderbach, L.; Van Buuren, T.; Sinclair, N.; Rigg, P. A.; Seifert, S.; Gog, T. Evolution of Carbon Clusters in the Detonation Products of the Triaminotrinitrobenzene (TATB)-Based Explosive PBX 9502. *J. Phys. Chem. C* **2017**, *121*, 23129–23140.
- (292) Kroto, H. W.; Heath, J. R.; O'Brien, S. C.; Curl, R. F.; Smalley, R. E.  $C_{60}$ : Buckminsterfullerene. *Nature* **1985**, *318*, 162–163.
- (293) McKinnon, J. T.; Bell, W. L.; Barkley, R. M. Combustion Synthesis of Fullerenes. *Combust. Flame* **1992**, *88*, 102–112.
- (294) Homann, K.-H. Fullerenes and Soot Formation - New Pathways to Large Particles in Flames. *Angew. Chem., Int. Ed.* **1998**, *37*, 2434–2451.
- (295) Jäger, C.; Huisken, F.; Mutschke, H.; Llamas Jansa, I.; Henning, T. Formation of Polycyclic Aromatic Hydrocarbons and Carbonaceous Solids in Gas-Phase Condensation Experiments. *Astrophys. J.* **2009**, *696*, 706–712.
- (296) Grieco, W. J.; Howard, J. B.; Rainey, L. C.; Vander Sande, J. B. Fullerene Carbon in Combustion-Generated Soot. *Carbon* **2000**, *38*, 597–614.
- (297) Bacsa, W. S.; de Heer, W. A.; Ugarte, D.; Châtelain, A. Raman Spectroscopy of Closed-Shell Carbon Particles. *Chem. Phys. Lett.* **1993**, *211*, 346–352.
- (298) de Heer, W. A.; Ugarte, D. Carbon Onions Produced by Heat Treatment of Carbon Soot and Their Relation to the 217.5 nm Interstellar Absorption Feature. *Chem. Phys. Lett.* **1993**, *207*, 480–486.
- (299) Ugarte, D. High-Temperature Behaviour of “Fullerene Black”. *Carbon* **1994**, *32*, 1245–1248.
- (300) Miki-Yoshida, M.; Castillo, R.; Ramos, S.; Rendón, L.; Tehuacanero, S.; Zou, B. S.; José-Yacamán, M. High Resolution Electron Microscopy Studies in Carbon Soots. *Carbon* **1994**, *32*, 231–246.
- (301) Ugarte, D. Curling and Closure of Graphitic Networks under Electron-Beam Irradiation. *Nature* **1992**, *359*, 707–709.
- (302) Terrones, M.; Terrones, G.; Terrones, H. Structure, Chirality, and Formation of Giant Icosahedral Fullerenes and Spherical Graphitic Onions. *Struct. Chem.* **2002**, *13*, 373–384.
- (303) Michelsen, H. A.; Tivanski, A. V.; Gilles, M. K.; van Poppel, L. H.; Dansson, M. A.; Buseck, P. R. Particle Formation from Pulsed Laser Irradiation of Soot Aggregates Studied with a Scanning Mobility Particle Sizer, a Transmission Electron Microscope, and a Scanning Transmission X-Ray Microscope. *Appl. Opt.* **2007**, *46*, 959–977.
- (304) Sorenson, C. M. The Mobility of Fractal Aggregates: A Review. *Aerosol Sci. Technol.* **2011**, *45*, 765–779.
- (305) Jacobson, M. Z. *Air Pollution and Global Warming: History, Science, and Solutions*, 2nd ed.; Cambridge University Press: New York, 2012; p 375.
- (306) Cheng, M.-D.; Corporan, E.; DeWitt, J. J.; Landgraf, B. Emissions of Volatile Particulate Components from Turboshaft Engines Operated with JP-8 and Fischer-Tropsch Fuels. *Aerosol Air Qual. Res.* **2009**, *9*, 237–256.
- (307) Zhang, H. X.; Sorenson, C. M.; Ramer, E. R.; Olivier, B. J.; Merklin, J. F. *In Situ* Optical Structure Factor Measurements of an Aggregating Soot Aerosol. *Langmuir* **1988**, *4*, 867–871.
- (308) Allen, T. *Particle Size Measurement*, 4th ed.; Chapman and Hall: London, 1990.
- (309) Sorenson, C. M.; Kim, W.; Fry, D.; Shi, D.; Chakrabarti, A. Observation of Soot Superaggregates with Fractal Dimension of 2.6 in Laminar Acetylene/Air Diffusion Flames. *Langmuir* **2003**, *19*, 7560–7563.
- (310) Kim, W.; Sorenson, C. M.; Chakrabarti, A. Universal Occurrence of Soot Superaggregates with a Fractal Dimension of 2.6 in Heavily Sooting Laminar Diffusion Flames. *Langmuir* **2004**, *20*, 3969–3973.
- (311) Kim, W.; Sorenson, C. M.; Fry, D.; Chakrabarti, A. Soot Aggregates, Superaggregates and Gel-Like Networks in Laminar Diffusion Flames. *J. Aerosol Sci.* **2006**, *37*, 386–401.
- (312) Dhaubhadel, R.; Pierce, F.; Chakrabarti, A.; Sorenson, C. M. Hybrid Superaggregate Morphology as a Result of Aggregation in a Cluster-Dense Aerosol. *Phys. Rev. E* **2006**, *73*, 011404.
- (313) Kearney, S.; Pierce, F. Evidence of Soot Superaggregates in a Turbulent Pool Fire. *Combust. Flame* **2012**, *159*, 3191–3198.
- (314) Chakrabarty, R. K.; Beres, N. D.; Moosmuller, H.; China, S.; Mazzoleni, C.; Dubey, M. K.; Liu, L.; Mishchenko, M. I. Soot Superaggregates from Flaming Wildfires and Their Direct Radiative Forcing. *Sci. Rep.* **2014**, *4*, 5508.
- (315) Chakrabarty, R. K.; Moosmüller, H.; Garro, M. A.; Stipe, C. B. Observation of Superaggregates from a Reversed Gravity Low-Sooting Flame. *Aerosol Sci. Technol.* **2012**, *46*, 1–3.
- (316) Kazemimanesh, M.; Moallemi, A.; Thomson, K. A.; Smallwood, G. J.; Lobo, P.; Olfert, J. A Novel Miniature Inverted-

- Flame Burner for the Generation of Soot Nanoparticles. *Aerosol Sci. Technol.* **2019**, *53*, 184–195.
- (317) Bambha, R. P.; Dansson, M. A.; Schrader, P. E.; Michelsen, H. A. Effects of Volatile Coatings on the Laser-Induced Incandescence of Soot. *Appl. Phys. B: Lasers Opt.* **2013**, *112*, 343–358.
- (318) Harris, S. J.; Maricq, M. M. Signature Size Distributions for Diesel and Gasoline Engine Exhaust Particulate Matter. *J. Aerosol Sci.* **2001**, *32*, 749–764.
- (319) Berg, M. J.; Sorensen, C. M. Internal Fields of Soot Fractal Aggregates. *J. Opt. Soc. Am. A* **2013**, *30*, 1947–1955.
- (320) Ortner, H. M. Sampling and Characterization of Individual Particles in Occupational Health Studies. *J. Environ. Monit.* **1999**, *1*, 273–283.
- (321) Fuller, K. A.; Malm, W. C.; Kreidenweis, S. M. Effects of Mixing on Extinction by Carbonaceous Particles. *J. Geophys. Res.* **1999**, *104*, 15941–15954.
- (322) Yon, J.; Bescond, A.; Ouf, F.-X. A Simple Semi-Empirical Model for Effective Density Measurements of Fractal Aggregates. *J. Aerosol Sci.* **2015**, *87*, 28–37.
- (323) Fuller, K. A. Scattering and Absorption Cross Sections of Compounded Sphere. II. Calculations for External Aggregation. *J. Opt. Soc. Am. A* **1995**, *12*, 881–892.
- (324) Sorensen, C. M.; Hageman, W. B.; Rush, T. J.; Huang, H.; Oh, C. Aerogelation in a Flame Soot Aerosol. *Phys. Rev. Lett.* **1998**, *80*, 1782–1785.
- (325) Sorensen, C. M.; Cai, J.; Lu, N. Light-Scattering Measurements of Monomer Size, Monomers Per Aggregate, and Fractal Dimension for Soot Aggregates in Flames. *Appl. Opt.* **1992**, *31*, 6547–6555.
- (326) Wentzel, M.; Gorzawski, H.; Naumann, K.-H.; Saathoff, H.; Weinbruch, S. Transmission Electron Microscopical and Aerosol Dynamical Characterization of Soot Aerosols. *J. Aerosol Sci.* **2003**, *34*, 1347–1370.
- (327) De Iuliis, S.; Cignoli, F.; Benecchi, S.; Zizak, G. Investigation of the Similarity of Soot Parameters in Ethylene Diffusion Flames with Different Heights by Extinction/Scattering Technique. *Symp. (Int.) Combust., [Proc.]* **1998**, *27*, 1549.
- (328) Palotás, A. B.; Rainey, L. C.; Feldermann, C. J.; Sarofim, A. F.; Vander Sande, J. B. Soot Morphology: An Application of Image Analysis in High-Resolution Transmission Electron Microscopy. *Microsc. Res. Tech.* **1996**, *33*, 266–278.
- (329) Köylü, Ü. Ö.; Faeth, G. M.; Farias, T. L.; Carvalho, M. G. Fractal and Projected Structure Properties of Soot Aggregates. *Combust. Flame* **1995**, *100*, 621–633.
- (330) Samson, R. J.; Mulholland, G. W.; Gentry, J. W. Structural Analysis of Soot Agglomerates. *Langmuir* **1987**, *3*, 272–281.
- (331) Sorensen, C. M. Light Scattering by Fractal Aggregates: A Review. *Aerosol Sci. Technol.* **2001**, *35*, 648–687.
- (332) Charalampopoulos, T. T.; Chang, H. Agglomerate Parameters and Fractal Dimension of Soot Using Light Scattering: Effects of Surface Growth. *Combust. Flame* **1991**, *87*, 89–99.
- (333) Oh, C.; Sorensen, C. M. The Effect of Overlap between Monomers on the Determination of Fractal Cluster Morphology. *J. Colloid Interface Sci.* **1997**, *193*, 17–25.
- (334) Gwaze, P.; Schmid, O.; Annegarn, H. J.; Andreae, M. O.; Huth, J.; Helas, G. Comparison of Three Methods of Fractal Analysis Applied to Soot Aggregates from Wood Combustion. *J. Aerosol Sci.* **2006**, *37*, 820–838.
- (335) Köylü, Ü. Ö.; Xing, Y. C.; Rosner, D. E. Fractal Morphology Analysis of Combustion-Generated Aggregates Using Angular Light Scattering and Electron Microscope Images. *Langmuir* **1995**, *11*, 4848–4854.
- (336) Bambha, R. P.; Dansson, M. A.; Schrader, P. E.; Michelsen, H. A. Effects of Volatile Coatings and Coating Removal Mechanisms on the Morphology of Graphitic Soot. *Carbon* **2013**, *61*, 80–96.
- (337) Brasil, A. M.; Farias, T. L.; Carvalho, M. G. A Recipe for Image Characterization of Fractal-Like Aggregates. *J. Aerosol Sci.* **1999**, *30*, 1379–1389.
- (338) Brasil, A. M.; Farias, T. L.; Carvalho, M. G. Evaluation of the Fractal Properties of Cluster-Cluster Aggregates. *Aerosol Sci. Technol.* **2000**, *33*, 440–454.
- (339) Brasil, A. M.; Farias, T. L.; Carvalho, M. G.; Köylü, Ü. Ö. Numerical Characterization of the Morphology of Aggregated Particles. *J. Aerosol Sci.* **2001**, *32*, 489–508.
- (340) Cross, E. S.; Onasch, T. B.; Aherne, A.; Wrobel, W.; Slowik, J. G.; Olfert, J.; Lack, D. A.; Massoli, P.; Cappa, C. D.; Schwarz, J. P.; Spackman, J. R.; Fahey, D. W.; Sedlacek, A.; Trimborn, A. M.; Jayne, J. T.; Freedman, A.; Williams, L. R.; Ng, N. L.; Mazzoleni, C.; Dubey, M.; Brem, B.; Kok, G.; Subramanian, R.; Freitag, S.; Clarke, A.; Thornhill, D.; Marr, L. C.; Kolb, C. E.; Worsnop, D. R.; Davidovits, P. Soot Particle Studies - Instrument Inter-Comparison - Project Overview. *Aerosol Sci. Technol.* **2010**, *44*, 592–611.
- (341) Ghazi, R.; Olfert, J. S. Coating Mass Dependence of Soot Aggregate Restructuring Due to Coatings of Oleic Acid and Diethyl Sebacate. *Aerosol Sci. Technol.* **2013**, *47*, 192–200.
- (342) Ghazi, R.; Tjong, H.; Soewono, A.; Rogak, S. N.; Olfert, J. S. Mass, Mobility, Volatility, and Morphology of Soot Particles Generated by a Mckenna and Inverted Burner. *Aerosol Sci. Technol.* **2013**, *47*, 395–405.
- (343) Johnson, T. J.; Symonds, J. P. R.; Olfert, J. Mass-Mobility Measurements Using a Centrifugal Particle Mass Analyzer and Differential Mobility Spectrometer. *Aerosol Sci. Technol.* **2013**, *47*, 1215–1225.
- (344) Johnson, T. J.; Olfert, J. S.; Symonds, J. P. R.; Johnson, M.; Rindlisbacher, T.; Swanson, J. J.; Boies, A. M.; Thomson, K. A.; Smallwood, G. J.; Walters, D.; Sevcenco, Y.; Crayford, A.; Dastanpour, R.; Rogak, S. N.; Durdina, L.; Bahk, Y. K.; Brem, B.; Wang, J. Effective Density and Mass-Mobility Exponent of Aircraft Turbine Particulate Matter. *J. Propul. Power* **2015**, *31*, 573–582.
- (345) Abegglen, M.; Durdina, L.; Brem, B. T.; Wang, J.; Rindlisbacher, T.; Corbin, J. C.; Lohmann, U.; Sierau, B. Effective Density and Mass-Mobility Exponents of Particulate Matter in Aircraft Turbine Exhaust: Dependence on Engine Thrust and Particle Size. *J. Aerosol Sci.* **2015**, *88*, 135–147.
- (346) Xue, H.; Khalizov, A. F.; Wang, L.; Zheng, J.; Zhang, R. Effects of Coating of Dicarboxylic Acids on the Mass-Mobility Relationship of Soot Particles. *Environ. Sci. Technol.* **2009**, *43*, 2787–2792.
- (347) Xue, H.; Khalizov, A. F.; Wang, L.; Zheng, J.; Zhang, R. Effects of Coating of Dicarboxylic Acids on the Mass-Mobility Relationship of Soot Particles. *Phys. Chem. Chem. Phys.* **2009**, *11*, 7869–7875.
- (348) Chakrabarty, R. K.; Moosmüller, H.; Arnott, W. P.; Garro, M. A.; Tian, G.; Slowik, J. G.; Cross, E. S.; Han, J.-H.; Davidovits, P.; Onasch, T. B.; Worsnop, D. R. Low Fractal Dimension Cluster-Dilute Soot Aggregates from a Premixed Flame. *Phys. Rev. Lett.* **2009**, *102*, 235504.
- (349) Pagels, J.; Khalizov, A. F.; McMurry, P. H.; Zhang, R. Processing of Soot by Controlled Sulphuric Acid and Water Condensation-Mass and Mobility Relationship. *Aerosol Sci. Technol.* **2009**, *43*, 629–640.
- (350) Kütz, S.; Schmidt-Ott, A. Characterization of Agglomerates by Condensation-Induced Restructuring. *J. Aerosol Sci.* **1992**, *23*, 357–360.
- (351) Saathoff, H.; Naumann, K.-H.; Schnaiter, M.; Schöck, W.; Möhler, O.; Schurath, U.; Weingartner, E.; Gysel, M.; Baltensperger, U. Coating of Soot and  $(\text{NH}_4)_2\text{SO}_4$  Particles by Ozonolysis Products of  $\alpha$ -Pinene. *J. Aerosol Sci.* **2003**, *34*, 1297–1321.
- (352) Bueno, P. A.; Havey, D. K.; Mulholland, G. W.; Hodges, J. T.; Gillis, K. A.; Dickerson, R. R.; Zachariah, M. R. Photoacoustic Measurements of Amplification of the Absorption Cross Section for Coated Soot Aerosols. *Aerosol Sci. Technol.* **2011**, *45*, 1217–1230.
- (353) Slowik, J. G.; Cross, E. S.; Han, J.-H.; Kolucki, J.; Davidovits, P.; Williams, L. R.; Onasch, T. B.; Jayne, J. T.; Kolb, C. E.; Worsnop, D. R. Measurements of Morphology Changes of Fractal Soot Particles Using Coating and Denuding Experiments: Implications for Optical Absorption and Atmospheric Lifetime. *Aerosol Sci. Technol.* **2007**, *41*, 734–750.

- (354) Witze, P. O.; Gershenson, M.; Michelsen, H. A. Dual-Laser LIDELOS: An Optical Diagnostic for Time-Resolved Volatile Fraction Measurements of Diesel Particulate Emissions. *SAE Technical Paper 2005-01-3791*; SAE: Warrendale, PA, 2005. DOI: 10.4271/2005-01-3791.
- (355) Zhang, R.; Khalizov, A. F.; Pagels, J.; Zhang, D.; Xue, H.; McMurry, P. H. Variability in Morphology, Hygroscopicity, and Optical Properties of Soot Aerosols During Atmospheric Processing. *Proc. Natl. Acad. Sci. U. S. A.* **2008**, *105*, 10291–10296.
- (356) Khalizov, A. F.; Xue, H.; Wang, L.; Zheng, J.; Zhang, R. Enhanced Light Absorption and Scattering by Carbon Soot Aerosols Internally Mixed with Sulfuric Acid. *J. Phys. Chem. A* **2009**, *113*, 1066–1074.
- (357) Miljevic, B.; Surawski, N. C.; Bostrom, T.; Ristovski, Z. D. Restructuring of Carbonaceous Particles Upon Exposure to Organic and Water Vapours. *J. Aerosol Sci.* **2012**, *47*, 48–57.
- (358) Dastanpour, R.; Rogak, S. N.; Graves, B.; Olfert, J.; Eggersdorfer, M.; Boies, A. M. Improved Sizing of Soot Primary Particles Using Mass-Mobility Measurements. *Aerosol Sci. Technol.* **2016**, *50*, 101–109.
- (359) Ono, K.; Dewa, K.; Matsukawa, Y.; Saito, Y.; Matsushita, Y.; Aoki, H.; Era, K.; Aoki, T.; Yamaguchi, T. Experimental Evidence for the Sintering of Primary Soot Particles. *J. Aerosol Sci.* **2017**, *105*, 1–9.
- (360) Nagle, J.; Strickland-Constable, R. F. Oxidation of Carbon between 1000–2000°C. *Proc. Fifth Conf. Carbon* **1962**, *1*, 154–164.
- (361) Neoh, K. G.; Howard, J. B.; Sarofim, A. F. Effect of Oxidation on the Physical Structure of Soot. *Symp. (Int.) Combust., [Proc.]* **1985**, *20*, 951–957.
- (362) Neoh, K. G.; Howard, J. B.; Sarofim, A. F. Soot Oxidation in Flames. In *Particulate Carbon*; Siegla, D. C.; Smith, B. W., Eds.; Plenum Press: New York, 1981; pp 261–277.
- (363) von Gersum, S.; Roth, P. Soot Oxidation in High Temperature N<sub>2</sub>O/Ar and NO/Ar Mixtures. *Symp. (Int.) Combust., [Proc.]* **1992**, *24*, 999–1006.
- (364) Stanmore, B. R.; Brilhac, J. F.; Gilot, P. The Oxidation of Soot: A Review of Experiments, Mechanisms, and Models. *Carbon* **2001**, *39*, 2247–2268.
- (365) Echavarria, C. A.; Jaramillo, I. C.; Sarofim, A. F.; Lighty, J. S. Studies of Soot Oxidation and Fragmentation in a Two-Stage Burner under Fuel-Lean and Fuel-Rich Conditions. *Proc. Combust. Inst.* **2011**, *33*, 659–666.
- (366) Mueller, M. M.; Blanquart, G.; Pitsch, H. Modeling the Oxidation-Induced Fragmentation of Soot Aggregates in Laminar Flames. *Proc. Combust. Inst.* **2011**, *33*, 667–674.
- (367) Sirignano, M.; Kent, J. H.; D'Anna, A. Further Experimental and Modelling Evidences of Soot Fragmentation in Flames. *Proc. Combust. Inst.* **2015**, *35*, 1779–1786.
- (368) Goldberg, E. D. *Black Carbon in the Environment: Properties and Distribution*; John Wiley & Sons: New York, 1985.
- (369) Bond, T. C.; Doherty, S. J.; Fahey, D. W.; Forster, P. M.; Berntsen, T.; DeAngelo, B. J.; Flanner, M. G.; Ghan, S.; Kärcher, B.; Koch, D.; Kinne, S.; Kondo, Y.; Quinn, P. K.; Sarofim, M. C.; Schultz, M. G.; Schulz, M.; Venkataraman, C.; Zhang, H.; Zhang, S.; Bellouin, N.; Guttikunda, S. K.; Hopke, P. K.; Jacobson, M. Z.; Kaiser, J. W.; Klimont, Z.; Lohmann, U.; Schwarz, J. P.; Shindell, D.; Storelvmo, T.; Warren, S. G.; Zender, C. S. Bounding the Role of Black Carbon in the Climate System: A Scientific Assessment. *J. Geophys. Res.* **2013**, *118*, 5380–5552.
- (370) Lack, D. A.; Moosmüller, H.; McMeeking, G. R.; Chakrabarty, R. K.; Baumgardner, D. Characterizing Elemental, Equivalent Black, and Refractory Black Carbon Aerosol Particles: A Review of Techniques, Their Limitations and Uncertainties. *Anal. Bioanal. Chem.* **2014**, *406*, 99–122.
- (371) Bond, T. C.; Bergstrom, R. W. Light Absorption by Carbonaceous Particles: An Investigative Review. *Aerosol Sci. Technol.* **2006**, *40*, 27–67.
- (372) Petzold, A.; Ogren, J. A.; Fiebig, M.; Laj, P.; Li, S.-M.; Baltensperger, U.; Holzer-Popp, T.; Kinne, S.; Pappalardo, G.; Sugimoto, N.; Wehrli, C.; Wiedensohler, A.; Zhang, X.-Y. Recommendations for Reporting “Black Carbon” Measurements. *Atmos. Chem. Phys.* **2013**, *13*, 8365–8379.
- (373) Sun, H.; Biedermann, L.; Bond, T. C. Color of Brown Carbon: A Model for Ultraviolet and Visible Light Absorption by Organic Carbon Aerosol. *Geophys. Res. Lett.* **2007**, *34*, L17813.
- (374) Corbin, J. C.; Czech, H.; Massabo, D.; de Mongeot, F. B.; Jakobi, G.; Liu, F.; Lobo, P.; Mennucci, C.; Mensah, A. A.; Orasche, J.; Pieber, S. M.; Prevot, A. S. H.; Stengel, B.; Tay, L.-L.; Zanatta, M.; Zimmermann, R.; El Haddad, I.; Gysel, M. Infrared-Absorbing Carbonaceous Tar Can Dominate Light Absorption by Marine-Engine Exhaust. *Clim. Atmos. Sci.* **2019**, *2*, 12.
- (375) Lack, D. A.; Bahreini, R.; Langridge, J. M.; Gilman, J. B.; Middlebrook, A. M. Brown Carbon Absorption Linked to Organic Mass Tracers in Biomass Burning Particles. *Atmos. Chem. Phys.* **2013**, *13*, 2415–2422.
- (376) Karanasiou, A.; Minguillon, M. C.; Viana, M.; Alastuey, A.; Putaud, J.-P.; Maenhaut, W.; Panteliadis, P.; Mocnik, G.; Favez, O.; Kuhlbusch, T. A. J. Thermal-Optical Analysis for the Measurement of Elemental Carbon (EC) and Organic Carbon (OC) in Ambient Air: A Literature Review. *Atmos. Meas. Technol. Discuss.* **2015**, *8*, 9649–9712.
- (377) Ogren, J. A.; Charlson, R. J. Elemental Carbon in the Atmosphere: Cycle and Lifetime. *Tellus, Ser. B* **1983**, *35B*, 241–254.
- (378) Moosmüller, H.; Chakrabarty, R. K.; Ehlers, K. M.; Arnott, W. P. Absorption Ångström Coefficient, Brown Carbon, and Aerosols: Basic Concepts, Bulk Matter, and Spherical Particles. *Atmos. Chem. Phys.* **2011**, *11*, 1217–1225.
- (379) Lack, D. A.; Langridge, J. M. On the Attribution of Black and Brown Carbon Light Absorption Using the Ångström Exponent. *Atmos. Chem. Phys.* **2013**, *13*, 10535–10543.
- (380) Schuster, G. L.; Dubovik, O.; Arola, A.; Eck, T. F.; Holben, B. N. Remote Sensing of Soot Carbon - Part 2: Understanding the Absorption Ångström Exponent. *Atmos. Chem. Phys.* **2016**, *16*, 1587–1602.
- (381) Forrister, H.; Liu, J.; Scheuer, E.; Dibb, J.; Ziembka, L.; Thornhill, K. L.; Anderson, B.; Diskin, G.; Perring, A. E.; Schwarz, J. P.; Campuzano-Jost, P.; Day, D. D.; Palm, B. B.; Jimenez, J. L.; Nenes, A.; Weber, R. J. Evolution of Brown Carbon in Wildfire Plumes. *Geophys. Res. Lett.* **2015**, *42*, 4623–4630.
- (382) Yang, M.; Howell, S. G.; Zhuang, J.; Huebert, B. J. Attribution of Aerosol Light Absorption to Black Carbon, Brown Carbon, and Dust in China - Interpretations of Atmospheric Measurements During East-Aire. *Atmos. Chem. Phys.* **2009**, *9*, 2035–2050.
- (383) Liu, C.; Chung, C. E.; Yin, Y.; Schnaiter, M. The Absorption Ångström Exponent of Black Carbon: From Numerical Aspects. *Atmos. Chem. Phys.* **2018**, *18*, 6259–6273.
- (384) Kirchstetter, T. W.; Novakov, T.; Hobbs, P. V. Evidence That the Spectral Dependence of Light Absorption by Aerosols Is Affected by Organic Carbon. *J. Geophys. Res.* **2004**, *109*, D21208.
- (385) Lack, D. A.; Cappa, C. D. Impact of Brown and Clear Carbon on Light Absorption Enhancement, Single Scatter Albedo and Absorption Wavelength Dependence of Black Carbon. *Atmos. Chem. Phys.* **2010**, *10*, 4207–4220.
- (386) O'Neill, N. T.; Eck, T. F.; Holben, B. N.; Smirnov, A.; Dubovik, O.; Royer, A. Bimodal Size Distribution Influences on the Variation of Angstrom Derivatives in Spectral and Optical Depth Space. *J. Geophys. Res.* **2001**, *106*, 9787–9806.
- (387) Donnet, J.-B.; Bansal, R. C.; Wang, M.-J. *Carbon Black*, 2nd ed.; Marcel Dekker, Inc.: New York, 1993.
- (388) Kushnir, D.; Sandén, B. A. Energy Requirements of Carbon Nanoparticle Production. *J. Ind. Ecol.* **2008**, *12*, 360–375.
- (389) Liu, H.; Ye, T.; Mao, C. Fluorescent Carbon Nanoparticles Derived from Candle Soot. *Angew. Chem., Int. Ed.* **2007**, *46*, 6473–6475.
- (390) Liu, C.; Singh, A. V.; Saggese, C.; Tang, Q.; Chen, D.; Wan, K.; Vinciguerra, M.; Commodo, M.; De Falco, G.; Minutolo, P.; D'Anna, A.; Wang, H. Flame-Formed Carbon Nanoparticles Exhibit Quantum Dot Behaviors. *Proc. Natl. Acad. Sci. U. S. A.* **2019**, *116*, 12692–12697.

- (391) Bottini, M.; Mustelin, T. Nanosynthesis by Candlelight. *Nat. Nanotechnol.* **2007**, *2*, 599–600.
- (392) Chandra, S.; Das, P.; Bag, S.; Laha, D.; Pramanik, P. Synthesis, Functionalization and Bioimaging Applications of Highly Fluorescent Carbon Nanoparticles. *Nanoscale* **2011**, *3*, 1533–1540.
- (393) Shaw, J. W. Smoke. *Am. Ind. Hyg. Assoc. Q.* **1950**, *11*, 49–50.
- (394) Simoneit, B. R. T. Biomass Burning: A Review of Organic Tracers for Smoke from Incomplete Combustion. *Appl. Geochem.* **2002**, *17*, 129–162.
- (395) Mulholland, G. W. Smoke Production and Properties. In *SFPE Handbook of Fire Protection Engineering*; DiNenno, P. J.; Beyler, C. L., Eds.; Society of Fire Protection Engineers: Quincy, MA, 2002; pp 258–268.
- (396) Colket, M. B. Particulate Formation. In *Gas Turbine Emissions*; Lieuwen, T., Yang, V., Eds.; Cambridge University Press: Cambridge, 2013; pp 123–153.
- (397) Watson, R. J.; Botero, M. L.; Ness, C. J.; Morgan, N. M.; Kraft, M. An Improved Methodology for Determining Threshold Sooting Indices from Smoke Point Lamps. *Fuel* **2013**, *111*, 120–130.
- (398) Paganini, E.; Mariotti, G.; Gasperetti, S.; Valletton, C.; Predolin, L.; Muré, E.; Palleschi, V.; Salvetti, A.; Tognoni, E. Multi-Diagnostic Approach to Characterize the Onset of Formation of Nanoparticles in a Premixed Laminar Ethylene/Air Flame. *Spectrochim. Acta, Part B* **2008**, *63*, 191–201.
- (399) Thierley, M.; Grotheer, H. H.; Aigner, M.; Yang, B.; Abid, A. D.; Zhao, B.; Wang, H. On the Existence of Nanoparticles Below the Sooting Threshold. *Proc. Combust. Inst.* **2007**, *31*, 639–647.
- (400) Minutolo, P.; Gambi, G.; D'Alessio, A.; D'Anna, A. Optical and Spectroscopic Characterization of Rich Premixed Flames across the Soot Formation Threshold. *Combust. Sci. Technol.* **1994**, *101*, 311–325.
- (401) Gill, R. J.; Olson, D. B. Estimation of Soot Thresholds for Fuel Mixtures. *Combust. Sci. Technol.* **1984**, *40*, 307–315.
- (402) Brown, N. J.; Revzan, K. L.; Frenklach, M. Detailed Kinetic Modeling of Soot Formation in Ethylene/Air Mixtures Reacting in a Perfectly Stirred Reactor. *Symp. (Int.) Combust., [Proc.]* **1998**, *27*, 1573–1581.
- (403) Bönig, M.; Feldermann, C.; Jander, H.; Lüters, B.; Rudolph, G.; Wagner, H. Gg. Soot Formation in Premixed C<sub>2</sub>H<sub>4</sub> Flat Flames at Elevated Pressure. *Symp. (Int.) Combust., [Proc.]* **1991**, *23*, 1581–1587.
- (404) Simonsson, J.; Olofsson, N.-E.; Hosseinnia, A.; Bengtsson, P.-E. Influence of Potassium Chloride and Other Metal Salts on Soot Formation Studied Using Imaging LII and ELS, and TEM Techniques. *Combust. Flame* **2018**, *190*, 188–200.
- (405) D'Alessio, A.; D'Anna, A.; Minutolo, P.; Sgro, L. A. Nanoparticles of Organic Carbon (NOC) Formed in Flames and Their Effects in Urban Atmospheres. In *Combustion Generated Fine Carbonaceous Particles*; Bockhorn, H., D'Anna, A., Sarofim, A. F., Wang, H., Eds.; KIT Scientific Publishing: Karlsruhe, Germany, 2009; pp 205–230. <https://publikationen.bibliothek.kit.edu/1000013744> (accessed September 2020-09-30).
- (406) Calcote, H. F.; Manos, D. M. Effect of Molecular Structure on Incipient Soot Formation. *Combust. Flame* **1983**, *49*, 289–304.
- (407) Yang, Y.; Boehman, A. L.; Santoro, R. J. A Study of Jet Fuel Sooting Tendency Using the Threshold Sooting Index (TSI) Model. *Combust. Flame* **2007**, *149*, 191–205.
- (408) Lemaire, R.; Therssen, E.; Desgroux, P. Effect of Ethanol Addition in Gasoline and Gasoline-Surrogate on Soot Formation in Turbulent Spray Flames. *Fuel* **2010**, *89*, 3952–3959.
- (409) Lemaire, R.; Lapalme, D.; Seers, P. Analysis of the Sooting Propensity of C-4 and C-5 Oxygenates: Comparison of Sooting Indexes Issued from Laser-Based Experiments and Group Additivity Approaches. *Combust. Flame* **2015**, *162*, 3140–3155.
- (410) McEnally, C. S.; Pfefferle, L. D. Improved Sooting Tendency Measurements for Aromatic Hydrocarbons and Their Implications for Naphthalene Formation Pathways. *Combust. Flame* **2007**, *148*, 210–222.
- (411) Das, D. D.; McEnally, C. S.; Pfefferle, L. D. Sooting Tendencies of Unsaturated Esters in Nonpremixed Flames. *Combust. Flame* **2015**, *162*, 1489–1497.
- (412) McEnally, C. S.; Pfefferle, L. D. Sooting Tendencies of Nonvolatile Aromatic Hydrocarbons. *Proc. Combust. Inst.* **2009**, *32*, 673–679.
- (413) McEnally, C. S.; Pfefferle, L. D. Sooting Tendencies of Oxygenated Hydrocarbons in Laboratory-Scale Flames. *Environ. Sci. Technol.* **2011**, *45*, 2498–2503.
- (414) Legros, G.; Wang, Q.; Bonnety, J.; Kashif, M.; Morin, C.; Consalvi, J.-L.; Liu, F. Simultaneous Soot Temperature and Volume Fraction Measurements in Axis-Symmetric Flames by a Two-Dimensional Modulated Absorption/Emission Technique. *Combust. Flame* **2015**, *162*, 2705–2719.
- (415) Khalghy, M. R.; Weingarten, J.; Sediako, A. D.; Barba, J.; Lapuerta, M.; Thomson, M. J. Structural Effects of Biodiesel on Soot Formation in a Laminar Coflow Diffusion Flame. *Proc. Combust. Inst.* **2017**, *36*, 1321–1328.
- (416) Das, D. D.; Cannella, W. J.; McEnally, C. S.; Mueller, C. J.; Pfefferle, L. D. Two-Dimensional Soot Volume Fraction Measurements in Flames Doped with Large Hydrocarbons. *Proc. Combust. Inst.* **2017**, *36*, 871–879.
- (417) Das, D. D.; McEnally, C. S.; Kwan, T. A.; Zimmerman, J. B.; Cannella, W. J.; Mueller, C. J.; Pfefferle, L. D. Sooting Tendencies of Diesel Fuels, Jet Fuels, and Their Surrogates in Diffusion Flames. *Fuel* **2017**, *197*, 445–458.
- (418) Saffaripour, M.; Thomson, K. A.; Smallwood, G. J.; Lobo, P. A Review on the Morphological Properties of Non-Volatile Particulate Matter Emissions from Aircraft Turbine Engines. *J. Aerosol Sci.* **2020**, *139*, 105467.
- (419) Peck, J.; Timko, M. T.; Yu, Z.; Wong, H.-W.; Herndon, S. C.; Yelvington, P. E.; Miake-Lye, R.; Wey, C.; Winstead, E. L.; Ziembka, L.; Anderson, B. E. Measurement of Volatile Particulate Matter Emissions from Aircraft Engines Using a Simulated Plume Aging System. *J. Eng. Gas Turbines Power* **2012**, *134*, 061503.
- (420) Krishnan, A.; Dujardin, E.; Treacy, M. M. J.; Hugdahl, J.; Lynum, S.; Ebbesen, T. W. Graphitic Cones and the Nucleation of Curved Carbon Surfaces. *Nature* **1997**, *388*, 451–454.
- (421) Naess, S. N.; Elgsaeter, A.; Helgesen, G.; Knudsen, K. D. Carbon Nanocones: Wall Structure and Morphology. *Sci. Technol. Adv. Mater.* **2009**, *10*, 065002.
- (422) Garberg, T.; Naess, S. N.; Helgesen, G.; Knudsen, K. D.; Kopstad, G.; Elgsaeter, A. A Transmission Electron Microscopy and Electron Diffraction Study of Carbon Nanodisks. *Carbon* **2008**, *46*, 1535–1543.
- (423) Kosky, P. G.; McAtee, D. S. An Experimental and Theoretical Investigation of Flame-Formed Diamonds. *Mater. Lett.* **1989**, *8*, 369–374.
- (424) Donnet, J.-B.; Oulanti, H.; Le Huu, T.; Schmitt, M. Synthesis of Large Single Crystal Diamond Using Combustion-Flame Method. *Carbon* **2006**, *44*, 374–380.
- (425) Hou, S.-S.; Chung, D.-H.; Lin, T.-H. High-Yield Synthesis of Carbon Nano-Onions in Counterflow Diffusion Flames. *Carbon* **2009**, *47*, 938–947.
- (426) Merchan-Merchan, W.; Saveliev, A. V.; Kennedy, L. A. Carbon Nanostructures in Opposed-Flow Methane Oxy-Flames. *Combust. Sci. Technol.* **2003**, *175*, 2217–2236.
- (427) Choucair, M.; Stride, J. A. The Gram-Scale Synthesis of Carbon Onions. *Carbon* **2012**, *50*, 1109–1115.
- (428) Vander Wal, R. L.; Ticich, T. M.; Curtis, V. E. Diffusion Flame Synthesis of Single-Walled Carbon Nanotubes. *Chem. Phys. Lett.* **2000**, *323*, 217–223.
- (429) Height, M. J.; Howard, J. B.; Tester, J. W.; Vander Sande, J. B. Flame Synthesis of Single-Walled Carbon Nanotubes. *Carbon* **2004**, *42*, 2295–2307.
- (430) Yuan, L.; Saito, K.; Hu, W.; Chen, Z. Ethylene Flame Synthesis of Well-Aligned Multi-Walled Carbon Nanotubes. *Chem. Phys. Lett.* **2001**, *346*, 23–28.